Development of Geopolymer-Based Cement and Soil Stabilizers for Transportation Infrastructure

Project No. 18CTAM03

Lead University: Texas A&M University

Collaborative Universities: University of Texas at Arlington

Final Report

September 2019

TECHNICAL DOCUMENTATION PAGE

1. Project No. 18CTAM03	2. Government Accession No.	3. Recipient's Catalog No.	
4. Title and Subtitle Development of Geopolymer-Based Cement and Soil Stabilizers for Transportation Infrastructure		**5. Report Date** Sept. 2019	
		6. Performing Organization Code	
7. Author(s) PI: Miladin Radovic https://orcid.org/0000-0003-4571-2848 Co-PI: Anand J. Puppala https://orcid.org/0000-0003-0435-6285		**8. Performing Organization Report No.**	
9. Performing Organization Name and Address Transportation Consortium of South-Central States (Tran-SET)		**10. Work Unit No. (TRAIS)**	
University Transportation Center for Region 6 3319 Patrick F. Taylor Hall, Louisiana State University, Baton Rouge, LA 70803		**11. Contract or Grant No.** 69A3551747106	
12. Sponsoring Agency Name and Address United States of America Department of Transportation Research and Innovative Technology Administration		**13. Type of Report and Period Covered** Final Research Report Mar. 2018 – Mar. 2019	
		14. Sponsoring Agency Code	

15. Supplementary Notes
Report uploaded and accessible at Tran-SET's website (http://transet.lsu.edu/).

16. Abstract

Geopolymer Cement (GPC) has drawn much attention in the recent years as an alternative to Ordinary Portland Cement (OPC) for soil stabilization, pavements, bridges and other transportation structures due to their good mechanical properties in comparison to OPC. In addition, GPC can be processed at room temperatures from aqueous solutions of waste materials (e.g. fly ash) or abundant natural sources (e.g. clay), thereby significantly reducing CO_2 production associated with processing of OPC. As such, GPC proves to be a more sustainable and environmentally friendly alternative than OPC. This research explores methods to develop GPC with desired properties and evaluate their durability characteristics as part of their long-term performance based on real service conditions when exposed to significant water intake during flooding or torrential rainfall. Teams from Texas A&M University (TAMU) and University of Texas at Arlington (UTA) collaborated in this study to understand GPC, propose different methods to synthesize GPC, and to effectively synthesize a GPC composition.

17. Key Words Geopolymer concrete, Carbon footprint, Pavements, Sustainability, Stabilization, Infrastructure	18. Distribution Statement No restrictions. This document is available through the National Technical Information Service, Springfield, VA 22161.		
19. Security Classif. (of this report) Unclassified	**20. Security Classif. (of this page)** Unclassified	**21. No. of Pages** 44	**22. Price**

Form DOT F 1700.7 (8-72)   **Reproduction of completed page authorized.**

SI* (MODERN METRIC) CONVERSION FACTORS

APPROXIMATE CONVERSIONS TO SI UNITS

Symbol	When You Know	Multiply By	To Find	Symbol
LENGTH				
in	inches	25.4	millimeters	mm
ft	feet	0.305	meters	m
yd	yards	0.914	meters	m
mi	miles	1.61	kilometers	km
AREA				
in^2	square inches	645.2	square millimeters	mm^2
ft^2	square feet	0.093	square meters	m^2
yd^2	square yard	0.836	square meters	m^2
ac	acres	0.405	hectares	ha
mi^2	square miles	2.59	square kilometers	km^2
VOLUME				
fl oz	fluid ounces	29.57	milliliters	mL
gal	gallons	3.785	liters	L
ft^3	cubic feet	0.028	cubic meters	m^3
yd^3	cubic yards	0.765	cubic meters	m^3
NOTE: volumes greater than 1000 L shall be shown in m^3				
MASS				
oz	ounces	28.35	grams	g
lb	pounds	0.454	kilograms	kg
T	short tons (2000 lb)	0.907	megagrams (or "metric ton")	Mg (or "t")
TEMPERATURE (exact degrees)				
^{o}F	Fahrenheit	5 (F-32)/9 or (F-32)/1.8	Celsius	^{o}C
ILLUMINATION				
fc	foot-candles	10.76	lux	lx
fl	foot-Lamberts	3.426	candela/m^2	cd/m^2
FORCE and PRESSURE or STRESS				
lbf	poundforce	4.45	newtons	N
lbf/in^2	poundforce per square inch	6.89	kilopascals	kPa

APPROXIMATE CONVERSIONS FROM SI UNITS

Symbol	When You Know	Multiply By	To Find	Symbol
LENGTH				
mm	millimeters	0.039	inches	in
m	meters	3.28	feet	ft
m	meters	1.09	yards	yd
km	kilometers	0.621	miles	mi
AREA				
mm^2	square millimeters	0.0016	square inches	in^2
m^2	square meters	10.764	square feet	ft^2
m^2	square meters	1.195	square yards	yd^2
ha	hectares	2.47	acres	ac
km^2	square kilometers	0.386	square miles	mi^2
VOLUME				
mL	milliliters	0.034	fluid ounces	fl oz
L	liters	0.264	gallons	gal
m^3	cubic meters	35.314	cubic feet	ft^3
m^3	cubic meters	1.307	cubic yards	yd^3
MASS				
g	grams	0.035	ounces	oz
kg	kilograms	2.202	pounds	lb
Mg (or "t")	megagrams (or "metric ton")	1.103	short tons (2000 lb)	T
TEMPERATURE (exact degrees)				
^{o}C	Celsius	1.8C+32	Fahrenheit	^{o}F
ILLUMINATION				
lx	lux	0.0929	foot-candles	fc
cd/m^2	candela/m^2	0.2919	foot-Lamberts	fl
FORCE and PRESSURE or STRESS				
N	newtons	0.225	poundforce	lbf
kPa	kilopascals	0.145	poundforce per square inch	lbf/in^2

TABLE OF CONTENTS

LIST OF FIGURES

LIST OF TABLES

ACRONYMS, ABBREVIATIONS, AND SYMBOLS

AASHTO	American Association of State Highway and Transportation Officials
ACerS	American Ceramics Society
ASTM	American Section of the International Association for Testing Materials
CH	High Plasticity Clay
CL	Low Plasticity Clay
DFW	Dallas-Fort Worth Metroplex
DSC	Differential Scanning Calorimetry
EDS	Energy Dispersive X-Ray Spectroscopy
FE-SEM	Field Emission Scanning Electron Microscopy
GP	Geopolymer
GPC	Geopolymer Cement
LL	Liquid Limit
MDD	Maximum Dry Density
MK	Metakaolin
NMR	Nuclear Magnetic Resonance
OMC	Optimal Moisture Content
OPC	Ordinary Portland Cement
PI	Plasticity Index
PL	Plasticity Limit
RH	Relative Humidity
RPM	Revolutions Per Minute
SEM	Scanning Electron Microscopy
TAMU	Texas A&M University
Tran-SET	Transportation Consortium of South-Central States
TRB	Transportation Research Board
TXDOT	Texas Department of Transportation
UCS	Unconfined Compressive Strength

USCS	Unified Soil Classification System
UTA	University of Texas at Arlington
XRD	X-Ray Diffraction

EXECUTIVE SUMMARY

Geopolymer Cement (GPC) has drawn much attention in the recent years as an alternative to Ordinary Portland Cement (OPC) for soil stabilization, pavements, bridges, and other transportation structures due to their beneficial mechanical properties in comparison to OPC. In addition, GPC can be processed at room temperatures from aqueous solutions of waste materials (e.g. fly ash) or abundant natural sources (e.g. clay), thereby significantly reducing CO_2 production associated with processing of OPC. This research explores methods to develop GPC with desired properties and evaluate their durability characteristics as part of their long-term performance based on real service conditions when exposed to significant water intake during flooding or torrential rainfall.

Teams from Texas A&M University (TAMU) and University of Texas at Arlington (UTA) collaborated in this study to understand GPC, propose different methods to synthesize GPC, and to effectively synthesize a GPC composition. A wide range of GPC compositions were tested for their UCS, shrinkage, water loss, density, and porosity after a 14-day curing period. The GPCs were tested to observe the effect of various compositional parameters such as SiO_2/Al_2O_3 ratio, water/solids ratio, and type of alkali cation. Even though these parameters have already been studied before, none has been done extensively for ambient-cured metakaolin (MK)-based GPC. While some compositions had very poor performance, others had performance comparable to that of OPC (e.g. Na421). It was observed that the open porosity is inversely correlated with density, however, denser samples do not always result in better UCS. Instead, GPC seems have an optimal density of ~1.5g/cm^3 for maximizing strength. Overall, Na-based pure GPC outperformed K-based pure GPC with better UCS and lower shrinkage.

Additionally, testing of GPC-treated subgrade soils was also conducted. GPC was applied to two subgrade soils at the application ratio of 4%, 10% and 15% by weight. One of them is classified as a low-plasticity clay and the other as a high-plasticity clay. Significant increase in compressive strength of geopolymer-treated soils was observed compared to untreated soils. It was observed that an increase in the geopolymer ratios increased the compressive strength of geopolymer-treated soils by 150-350% for the low-plasticity clay and by 90-400% for the high-plasticity clay over a period of 0 (6 hours), 7, and 28 days.

Significant reduction in mass increase during 24-hour capillary soaking is observed in GPC-treated soil as compared to untreated soil. The untreated high-plasticity soil was observed to soak up more water than the untreated low-plasticity clay, although upon treatment with geopolymers the high-plasticity clay reduces intake of water considerably in comparison with the low-plasticity clay. Appropriate reduction in mass gain is obtained by the seventh day of curing in both soil-types. The 4% GPC is observed to be sufficient to significantly reduce mass change in the low-plasticity clay, while the 10% GPC ratio is observed to be more appropriate for significant decrease in mass change for the high-plasticity clay.

The soils treated with the higher amount of GPC have higher pH in the range of 12-13 for both soils. The pH of geopolymer-treated soils decreases by about 6-8% over a period of 28 days. The

geopolymer-treated low-plasticity clay is observed to have slightly higher pH than the similar geopolymer treated high-plasticity clay. The pH of geopolymer-treated soils dips below the lime cut-off pH of 12.4 more rapidly in high-plasticity clay at 21 days than in the low-plasticity clay at 28 days.

The performance of GPC-treated soil clearly demonstrates its effectiveness in stabilizing clayey soils, thereby increasing strength and mitigating volume changes during 1D-swell and shrinkage tests. It was interesting to observe the rate of increase of strength of geopolymer-treated soils, which show potential to be used as stabilizers where the time for construction is very limited and lowest cost of stabilization is not essential. Future studies on other problematic soils are suggested prior to be considered for field implementation.

Last but not least, a significant improvement in strength is observed when sand is added to GPC for the formation of GPC mortar samples. It's interesting to note that the best performing GPC did not necessarily result in the best performing GPC mortar. Instead, all the GPC mortar with low water content and high SiO_2/Al_2O_3 ratio has similar UCS of ~30 MPa (4,300 psi). The GPC mortar samples were also observed to have low and improved shrinkage even for those made from GPC that had significantly high value of shrinkage (e.g. K421, and K431).

Overall, pure ambient-cured MK-based GPC were demonstrated to have properties comparable to that of commercially available OPC. It was interesting to observe the improvement in properties notably UCS and shrinkage when sand is added to the system. Further studies on compositional effect, and structural characterizations are suggested to improve the competitiveness of GPC.

1. INTRODUCTION

Over the last several of years, a new class of alumino-silicate-polymers, commonly referred to as Geopolymers has received much attention as an eco-friendly and sustainable alternative to Ordinary Portland Cements (OPC) *(1-3)*. Geopolymers (GPs) harden at ambient temperatures in a relatively short amount of time *(4)* and can be synthesized by curing activated solutions of various alumino-silicate sources including natural minerals (e.g. clay), their products (e.g. metakaolin), and waste materials (e.g. fly ash, furnace slag, etc.). GPs are known for their high compressive strength and low shrinkage properties. GPs have a much lower carbon footprint than lime and OPC *(5)*, and is therefore more environmentally friendly than other conventional additives used for soil stabilization.

Geopolymer cements (GPCs) or binders has been investigated and/or used as alternative cementitious material for soil stabilization, pavements, bridges, and other transportation structures. Great interest in GPCs resides on the fact that they can be processed at room temperatures from aqueous solutions of waste materials (e.g. fly ash) or abounded natural sources (e.g. clay and other minerals) using , in best case scenario, only 10% of the energy required to make OPC *(1)*. Recent studies on the life-cycle analysis of GPC discusses the complications behind clearly quantifying the eco-friendliness of GPC due to the wide range of potential feedstock sources: when compared to OPC, GPC can range from 97% lower to 14% higher in terms of emission *(6, 7)*. However, an issue of particular importance is the lack of service history and absence of data on durability performance of GPC products, while OPC has been used for over 200 years. The later makes it clear that broader application of GPCs in transportation infrastructure requires further investigation on durability of different GPC structures. This report covers the work on durability of GPC concrete/mortar and GPC stabilized base and subgrade materials during long-term exposure to the service conditions typical for Region 6, especially during flooding and extreme rainfalls, to foster use of this new class of sustainable and eco-friendly materials for transportation infrastructure in Region 6. In addition, long-term performance testing of Geopolymer-treated subgrade soils is also studied. The use of sustainable materials or technology is highly encouraged to promote eco-friendly construction of various types of infrastructure including pavements *(8-13)*. Hence, use of geopolymer, which is an eco-friendly product may be considered as a green solution.

2. OBJECTIVES

The overall objective of this study is to develop an innovative, sustainable, eco-friendly and durable GPC for transportation infrastructure in Region 6, more specifically for GPC for concrete/mortar structures (pavements, bridges, etc.) and stabilization of base and subgrade foundation support for pavements, using natural and waste materials that abound in the region.

More specific objectives of the research are to:
- Select composition of GPC with optimum workability and mechanical properties;
- Characterize degradation of their structure and properties in condition simulating real weather conditions typical for Region 6, such as flooding, heavy rainfall or drought using extensive durability testing;
- Conduct leachability studies, to study the volume of leachate generated and its chemical composition;
- Provide guidance for the optimum composition of GPCs for extended durability of concrete/mortar structures and stabilized soil; and
- Implement research results and develop the workforce with the expertise in using novel technologies for soil stabilization.

3. LITERATURE REVIEW

The term 'Geopolymers' was coined by Joseph Davidovits in the 1970s for alumino-silicate polymers synthesized from rock-forming minerals *(1)*, which were used as fire-resistant coating materials. This initial work was then expanded and is now present in various applications such as: fire protection for cruise ship *(14)*, resin of high-temperature carbon-fiber composite *(15)*, thermal protection for wooden structure *(16)*, and more *(6)*. Moreover, geopolymers have been further developed and now find a wide range of applications such as: construction material alternative to OPC *(6)*, nuclear waste immobilization *(17)*, water purification (heavy metal immobilization) *(17)*, and low-energy processing route to ultra-refractory ceramics powder (such as SiC and Si_3N_4) *(18)*. Geopolymer has often been hailed as the next-generation "green" alternative to OPC, however, this claim has not been properly backed up. In general, most of the geopolymer studies back up the claim with the significant reduction in CO_2 emission as some of the environmental evaluation of geopolymer does as well *(19, 20)*. However, as stated in Provis and Van Deventer's book *(6)*, life cycle analysis is much more than just evaluating the greenhouse gas emission (also referred to as global warming potential, GWP). There are also several other important parameters to evaluate in a life cycle analysis such as: depletion of resources, acidification, human toxicity…etc. The more completed studies *(6, 7)* that do look at all the parameters were both able to demonstrate the benefits of using geopolymer for their specified application and local conditions, but neither drew very definite conclusions. Instead, they concluded that the result will vary a lot case-by-case since geopolymer is a very complicated system that has a wide range of feedstock material, and many of these materials do not have well-established means of transportation either.

During the geopolymerization process, reactive alumino-silicate minerals dissolve in highly alkaline solutions in the presence of an alkali hydroxide and silicate solution to form common Si and Al species, which in turn form chains of Al-O-Si and Si-O-Si bonds during a polycondensation process during which water is expelled *(1)*. The polycondensation process continues to develop 3-D net like features, and ultimately into an amorphous rigid gel known as geopolymer *(3)*. Previous research shows that GP-stabilized soil has unconfined compression strength (UCS) values ranging from 2-7 MPa after 7 days of curing *(2, 21)*. However, it is difficult to reproduce these results due to the differences in both soil and precursor (e.g. fly ash) composition. Additionally, most methodologies from existing literature are heavily application-driven and does not thoroughly explore the fundamental science behind the results. It has proved challenging to create an experimental procedure that would allow a systematic study to thoroughly understand how the different parameters affect GP's effectiveness as a soil stabilizer efficiently. In both papers by Zhang et al. *(3, 21)* the group conducted well-organized studies on GP's effectiveness as a soil stabilizer, with the first paper finding an effective amount by focusing on mechanical properties, and the second paper further investigating other engineering soil properties at and around the effective amount. It is evident from previous literature that GP works as soil stabilizer and is superior to OPC and lime in terms of durability, but still lacks the attraction due to coming up short in terms of mechanical properties. Based on the review of literature, it is suggested that the usage of GP as soil stabilizer would be more attractive if the same mechanical properties can be achieved while utilizing equal or lesser amount of GP to that of OPC and lime. We have followed Zhang et al.'s *(3, 21)* work by starting out with metakaolin since their work contains the most description in methodology, and it is the better choice to gain fundamental understandings on how GP work as soil stabilizers.

Many parts of US, including region 6 have many issues due to low strength and high swell-shrinkage characteristics of expansive soils *(22-27)*. Excessive droughts often cause significant cracking at the surface of embankments and pavements *(28-30)*. Various traditional chemical and some non-traditional stabilization techniques have been used in Region 6 and around the world to mitigate these issues *(31-39)*. Texas and its surrounding states experience cycles of intense droughts and flooding, which induces significant volume changes and pavement distress *(10, 37, 40)*. Durability studies attempt to replicate real-world climate scenarios, so long-term performance of treated soils and cement mixtures can be understood more realistically. Several studies have been conducted on the durability testing of lime-treated soil, especially in Texas *(41)*. The Texas Department of Transportation (TXDOT) has its own standards on conducting durability testing on lime-treated soil. On the other hand, there are very few studies conducted that have determined the durability of geopolymers or geopolymer-treated soil. A fly-ash based geopolymer submerged in a sulfuric acid-water solution (1:4 ratio) having pH =3.0 for a period of 120 days and was found to have a 40% decrease in unconfined compressive strength *(42)*. Another study conducted durability tests as per ASTM D559 for fly ash-based geopolymer-treated soil and observed that it lasted for about 11 cycles *(43)*.

Although GPC concrete has been of interest since the early 2000s *(44-46)* and achieved strength that is on par with OPC concrete, a very limited work has been done on GPC processed from metakaolin and GPC mortar which only uses fine aggregate such as sand. The late is especially important for transportation infrastructure as GPC can be used as a pavement when mixed with sand, or for stabilization of sand rich soil or subgrade. From the report summarized by Shayan in 2016, most of the studies since then focuses on optimizing fly ash-based GPC concrete as well as the usage of elevated temperature curing *(47)*, which are not ideal studies for implementation and commercialization. It is interesting to note that there's a study that claim elevated temperature curing is viable for implementation since geopolymerization is an exothermic reaction, and when processing larger samples it will practically be self-heating *(48)*. That being said, a construction company (Wagners) in Australia built an airport using GPC concrete using slag and fly ash as the precursor. This major project was made possible with 40,000 m^3 of GPC concrete, however, it also took ~10 years of research and development *(49)*. Even though utilizing fly ash increases the economic and environmental appeal, the variation of fly ash from source to source impacts the reproducibility of the results. In addition, increasing demand and prices of fly ash, tougher with its limited availability, makes metakaolin more attractive precursor material for GPC.

Metakaolin (MK)-based GPC have been extensively studied to gain a better understanding of GPC on the fundamental level since it is a pure aluminosilicate source, which allows reproducibility regardless of source, for example: physical evolution with temperature *(50-52)*, formation of crystalline phases *(53, 54)*, and nuclear magnetic resonance (NMR) studies *(55)*. Even so there are only a handful studies on mechanical properties *(50, 51, 56-60)* or long-term durability *(61, 62)* utilizing MK-based GPC compared to similar studies utilizing fly ash (FA)-based GPC. Few are actually well-organized, and the conclusions do not always agree across the studies. Recent studies suggest that wet-dry cycle of GPC could potentially affect durability of the GPC concrete structures *(47, 61, 63, 64)* and stabilized soil due to carbonation reaction (reaction with ambient CO_2 in humid environment or high water content) *(65-68)*, decomposition and leaching of the alkali activators *(64, 69-73)*, alkali-aggregate reaction *(64, 72, 74)*, volumetric changes and micro-cracking *(75)*, etc. Reaction of GPC with environmental water not only affects durability of GPC products, but also could potentially have deleterious environmental effects due to leaching of alkali

activators from GPC into surrounding *(70)*. Based on the limited studies from existing literature, there's a need for a comprehensive parametric study that can be served as a baseline guidance for future GPC studies. Hence, this report will present a novel study to extensively study the effects of varying chemical composition parameters on MK-based GPC for pavement infrastructure.

4. METHODOLOGY

The primary focus of this research is to develop GPC with desired properties and to evaluate the long- term performance of GPC and GP-treated soils in real service conditions found in Region 6. To this end, the research was categorized into five tasks: (1) synthesis and characterization of GP, (2) material development and characterization of GPC, (3) characterization of different soils typical for Region 6, (4) GP treatment of soils, and (5) long-term performance testing of geopolymer treated soil, and (6) characterization of GPC/sand. The following sections detail the procedures and outcomes of the tasks conducted to synthesize GPC and evaluate their long-term performance.

4.1. Synthesis and Characterization of GP

The GPs used in this research were synthesized by researchers using sodium or potassium hydroxide (Mallinckrodt Chemicals, NJ), amorphous fumed silicon (IV) oxide (Alfa Aesar, MA) with 350- 410 m^2/g specific surface area, MetaMax® (BASF Catalysts LLC, NJ) metakaolin, and deionized water. Metakaolin is a purer alumino-silicate source than the more commonly used fly ash with higher impurities and was therefore used as a precursor for GP synthesis in this research.

The sodium or potassium hydroxide was dissolved in deionized water to create a highly alkaline solution to process the alkali metal cations. The amorphous fumed silicon oxide was then added to adjust the SiO_2/Al_2O_3 ratio of the final product as desired, to create the activating solution for the synthesis of geopolymer. The activating solution was then mixed with metakaolin, which is a high-purity activating aluminosilicate source in a high-sheared mixer for 6 minutes at 400 revolutions per minute (RPM) to create a homogenized mixture, known as GP.

4.2. Material Development and Characterization of GPC

4.2.1. Parametric Study of GPC and GPC/Sand

The framework behind the development of GPC for Group 1 and Group 2 samples in the Task 1 is based on previous work by Lizcano et al. *(4)*, in which the samples are small in size (i.e., 1 in. x 1 in. cylinders) that allows a comprehensive parametric study of GPC composition to better understand the correct direction to maximize compressive strength. The important differences between this work and Lizcano et al. is that this study will evaluate the performance of both pure GPC binder samples and GPC/sand samples with varying percentages of testing sand according to ASTM C778 *(76)* while all curing under ambient temperature as oppose to elevated temperature. The second part of this study will then select few of the optimized compositions and test them according to ASTM C109 (2 in. cubes) *(77)* for better comparison to existing studies. However, the purpose of this study is to serve as a baseline and guidance for all future GPC mortar/concrete and GP soil stabilization studies. Therefore, the chosen raw materials and procedure have a heavy emphasis on reproducibility. Note that a total of 16 sets of pure GPC and GPC/sand and GPC soil samples with different composition were synthesized and tested instead of the proposed 8 set of samples (samples in Group 1 and Group 2). The 16 compositions are chosen to investigate the effect of cation (Na vs. K), SiO_2/Al_2O_3 ratio (2-4), and the water/solids ratio. Note that all GPC samples with different compositions are labeled as KXYZ or NaXYZ, where the first letters denote potassium (K) or sodium (Na) while XYZ numbers denote SiO_2/Al_2O_3 ratio, water to solid ratio used to prepare GPC, and Na/Al or K/Al ratio respectively. For example, GPC sample K421 is

sample prepared with K-activator, and $SiO_2/Al_2O_3=4$, water/solid ratio=2, and K/Al=1. All the compositions used throughout the different studies are listed and summarized below in Table 1.

Table 1. List of all GP compositions used throughout the different studies.

Composition	Pure GPC + GPC/Sand Study	GP/CL Study	GP/Soil Durability
Na241	x		
Na251	x		
Na(2.5)31	x		
Na(2.5)41	x		
Na321	x		
Na331	x		
Na341	x		
Na421	x		
Na431	x		
Na441	x		
K231	x		
K241	x		
K(2.5)21	x		
K(2.5)31	x		
K321	x		
K3(2.5)1		x	
K331	x		
K(3.5)(2.23)1		x	
K421	x	x	
K431	x	x	x
K441	x	x	
K(4.5)(1.82)1		x	

For GPC/sand samples, pure GPC was manually mixed with testing sand in the proportion amount varying from low percentage to standard percentage in terms of dry GPC to dry sand ratio, i.e. from 8% to 27% GPC into sand in a mixing bowl then the mixture was poured and manually compacted into 1 in. x 1 in. plastic cylindrical molds. Note that 27% GPC in sand has the same binder to sand ratio as standard OPC mortar according to ASTM C109 (1-part OPC with 2.75-part sand) *(77)*.

The samples' dimensional and weight change throughout the curing process was documented to measure shrinkage and water loss. Shrinkage was calculated by assuming initial dimension of the sample is the same as the inner dimension of the mold, and the diameter of the sample is taken as the average of 3 measurements. The density and open porosity of the samples was measured through Archimedes' principle after 7 days of curing in a sealed environment then demolded and dried for another 7 days in ambient conditions. Density and open porosity were calculated with Equations 1 and 2 as specified in ASTM C830-00 *(78)*. To measure m_{wet}, the samples were submerged in 200 proof ethanol, and placed into a vacuumed desiccator for 20 minutes. The samples were then removed, and the surface was dried with cloth towel to remove excess ethanol before measurement. The samples were then left in ambient condition for a day so the ethanol

would evaporate, after which they were tested with an 810 Materials Testing System (MTS System Corporation, MN) in compression mode with constant displacement rate of 0.60 mm/min.

$$\rho = \frac{m_{dry}*\rho_{ethanol}}{m_{wet}-m_{suspended}+m_{wire}}$$ [1]

where:
ρ = Measured density (g/cm^3);
m_{dry} = Dry mass (g);
$\rho_{ethanol}$ = Density of ethanol (g/cm^3);
m_{wet} = Mass of sample with ethanol occupying the open pores (g);
$m_{suspended}$ = Mass of sample while suspended in ethanol (g); and
m_{wire} = Mass of the part of Archimedes' set up that's used to suspend sample in ethanol (g).

$$P_{open} = \frac{m_{wet}-m_{dry}}{m_{wet}-m_{suspended}+m_{wire}} * 100\%$$ [2]

where:
P_{open} = Open porosity (%).

For comparison, small OPC samples were also processed using TXI Portland Cement Type I/II mix (TXI, TX) purchased from Home Depot using water/solids weight ratio of 0.42. All processing and characterization of OPC samples were kept consistent with GPC samples for best comparison.

After the comprehensive parametric studies, the best performing, and the worst performing compositions will be selected for materials characterizations such as SEM, EDS, and NMR to get a better understanding of the underlying mechanisms behind the difference in properties. SEM analyses of all samples were carried out with the JEOL JSM-7500F (JEOL USA Inc, MA) FE-SEM to study the microstructure of the samples. The characterized samples were not sputtered and characterized under low voltage to obtain the best representative morphology.

4.2.2. Long-Term Performance Testing of GPC

Once the parametric study on the UCS of GPC and GPC mortar is completed. The optimized compositions will be selected, and the samples will be processed to follow the sample size requirement for long-term performance test such as leaching and wet/dry cycle as proposed in Task 3. No result is presented for this portion since the study is still in progress.

4.3. Soil Characterization

Two expansive clay subgrade soils commonly found in North Texas were obtained from Lewisville, TX and Alvarado, TX to be stabilized with GP. The main criterion for the selection of subgrade soils was based on their Plasticity Index (PI), which ranges between 10 to 60, ensuring the expansive characteristic of the soils. All subgrade soil testing was conducted on oven-dried, crushed and pulverized soil.

Based on the particle size distribution tests, the clay from Lewisville, TX of the Eagle Ford geological formation was classified as a high-plasticity clay (CH), while the clay obtained from Alvarado, TX was classified as a low-plasticity clay (CL) as shown in Table 2.

Table 2. Summary of gradation tests: Sieve analysis and hydrometer tests.

Soil Location	Gravel	Sand	Silt	Clay	USCS Classification
Lewisville	0.0%	9.8%	34.3%	56.0%	CH
Alvarado	0.0%	33.6%	33.9%	32.5%	CL

The Atterberg limits, which include the liquid limit (LL), plastic limit (PL), and PI of the cohesive subgrade soils, were determined on the soil fraction that passes the 425-µm (No. 40) sieve (see Table 3), as per ASTM D4318-17 *(79)*. The specific gravity tests of the two untreated soils of this study were conducted as per ASTM D854-14 *(80)* and determined using a water pycnometer of soils passing the 4.75 mm (No. 4) sieve. The Atterberg limits and specific gravity values of the selected soils are shown in Table 3 and are found to be consistent with the expected values. Note that CH has a very high LL of 80% yielding a significantly high PI of 53%, while CL has a PI of 17% that just qualifies the soils as highly plastic.

Table 3. Summary of Atterberg limits and specific gravity tests.

Soil Type	LL (%)	PL (%)	PI (%)	G_S
CH	80	27	53	2.78
CL	42	25	17	2.69

Moisture-density relationships of untreated soils were determined using standard proctor and Harvard Miniature compaction tests, as per ASTM D698-12 *(81)* and GR-84-14 *(82)* respectively. The compaction tests were conducted to determine the optimum moisture content (OMC) at which the soils are compacted to its maximum dry density (MDD). The compaction test results of the two untreated soils are given in Table 4. Note that, as expected CL has a higher MDD and lower OMC than CH.

Table 4. Summary of moisture-density relationship tests of untreated soils.

Soil Type	MDD (g/cm^3)	OMC (%)
CH	1.57	24.2
CL	1.72	19.9

X-ray diffraction (XRD) and X-ray fluorescence (XRF) were performed on both subgrade soils to identify the mineral and chemical compositions. XRD scan was done using Siemens D5000matic system (Siemens AG, Germany) equipped with a ceramic copper tube. The samples were prepared by first grinding to ~400 mesh then packed into a plastic holder and scanned over the range of 3-61° 2θ using Cu-Kα radiation. Both the XRD scan and analyses (Table 5) were done through the service of The Mineral Lab (Golden, CO). XRF scan was done using Rigaku Supermini200 (Rigaku Corporation, Japan), and each sample was scanned twice for qualitative and quantitative information (Table 6). As the name implies, qualitative scan gives a rough idea of the chemical composition of sample, but cannot detect light elements properly, hence the lack of Na_2O. Quantitative scan gives a more accurate composition, but for each elements a standard is needed to obtain the data. Since we do not have a standard for TiO_2, the quantity for it is missing.

Table 5. Mineral composition of soils from XRD.

Mineral Name	Chemical Formula	CL (%)	CH (%)
Quartz	SiO_2	43	14
Calcite	$CaCO_3$	40	17
Kaolinite	$Al_2Si_2O_5(OH)_4$	<5	5
Smectite	$(Ca,Na)_x(Al,Mg,Fe)_4(Si,Al)_8O_{20}(OH,F)_4 \bullet (OH,F)_2$	<10	38
Mica/illite	$(K,Na,Ca)(Al,Mg,Fe)_2(Si,Al)_4O_{10}(OH,F)_2$	-	18
Plagioclase feldspar	$(Na,Ca)Al(Si,Al)_3O_8$	<3?	<5
K-feldspar	$KAlSi_3O_8$	<5	<3?
Anatase	TiO_2	-	<2?
"Unidentified"	?	<5	<5

Table 6. Chemical composition of soils from XRF.

CL (wt%)									
	MgO	Al_2O_3	SiO_2	SO_3	K_2O	CaO	TiO_2	Fe_2O_3	Na_2O
Qual	1.08	15.10	46.36	0.12	1.38	27.47	1.17	7.32	-
Quan	0.83	15.88	42.85	-0.21	1.04	20.28	-	4.57	0.09
CH (wt%)									
	MgO	Al_2O_3	SiO_2	SO_3	K_2O	CaO	TiO_2	Fe_2O_3	Na_2O
Qual	1.70	20.57	50.67	1.33	2.83	10.54	1.35	11.02	-
Quan	1.51	19.91	50.72	0.50	2.51	9.25	-	9.95	0.24

4.4. Geopolymer-Treatment of Soils

Since GP has multiple parameters (i.e. chemical composition, curing time and temperature) that depend on each other, the preliminary study primarily determined the relationship between mixability and water ratio for both sodium and potassium-based GP. It is worth noting that increasing water and silica content decreases viscosity and increases curing time, and that sodium-based GP are more viscous than potassium-based GP at the same water content. Taking into account all these different parameters as well as the mechanical properties from Lizcano et al. *(4)*, it was decided that GP with molar ratio of Si/Al = 2 and Al/K = 1 (GP-ID: K421, K431, K441) would produce the best candidates to maximize both strength and mixability/workability for soil stabilization. The details regarding the synthesis process has also been published by the authors *(83, 84)*.

The K431 GP mix was used to stabilize both selected soils at ratios of 4, 10, and 15% by weight of metakaolin to dry soil as proposed in Task 2 Group 3. Water was initially added to dry soil to bring it to its OMC, then covered and placed in a moisture room overnight so the moisture equilibrates throughout the soil. Once the soil was removed from the moisture room, the GP mixture at its appropriate ratio was added to the soil at OMC and mixed thoroughly. All treated soils were compacted at the OMC of the respective soil-GP mixtures and to 95% of their MDD. Treated samples were cured for a period of 0 (6-hour), 7 and 14 days and tested for durability. Curing of GP-treated soil was undertaken in a moisture room at 100% RH. Unconfined compressive strength, and pH tests were conducted on geopolymer-treated soil samples.

However, it is still worth to investigate effect of each parameters in the GP-soil system. Therefore, parametric study is carried out to observe the effect of each parameters on UCS with CL. The

parameters include %MK, cation (Na vs. K), Si/Al ratio, H_2O/Solids ratio in GP, and total H_2O % (to dry soil). All the samples done in this parametric study are cylindrical with dimension of roughly 1 in. diameter by 2 in. height and have been cured at room temperature at 100% relative humidity (RH) for 7 days before testing. This study actually goes beyond the scope of what was proposed, since various clay minerals have been shown to geopolymerize in alkaline environment using either NaOH or KOH (85). Therefore, it would be critical to show how the baseline study done from Subsection 4.2.1. applies to a more complicated system.

4.5. Long-Term Performance Testing of Geopolymer-Treated Soil

4.5.1. Durability Testing

Durability testing of soil-cement mixtures is usually conducted as per ASTM D559 method (86), where specimens are subjected to alternating cycles of wetting and drying to see how they perform in the long run. Soil-cement mixture are compacted to 95% of their MDD at their OMC and cured in a moisture-control room for seven days. After the seven-day curing period, the soil-cement mixtures are subjected to wet-dry cycles. For each wet-dry cycle, the specimen is submerged in water for a period of 5 hours and then placed in an oven at 70°C for 48 hours. This wetting and drying process is repeated for 12 cycles. After each wetting or drying cycle, the specimen is weighed, and its dimensions measure to mass and volume change respectively. In addition, the specimen is also brushed with a wire-scratch brush to estimate soil-cement loss.

Geopolymer-treated soil specimens were tested as per the ASTM D559 standards (86), although they disintegrated during the first wetting cycle. As such, an alternative method known as the capillary soaking method was undertaken to address the effect of ingress of water into geopolymer-treated specimen as part of durability testing for Task 3. The capillary soaking setup consisted of a container filled with coarse-grained sand filled with water up to the top of the sand layer (Figure 1). A porous stone is placed on the water-filled sand and the soil specimen placed atop the porous stone.
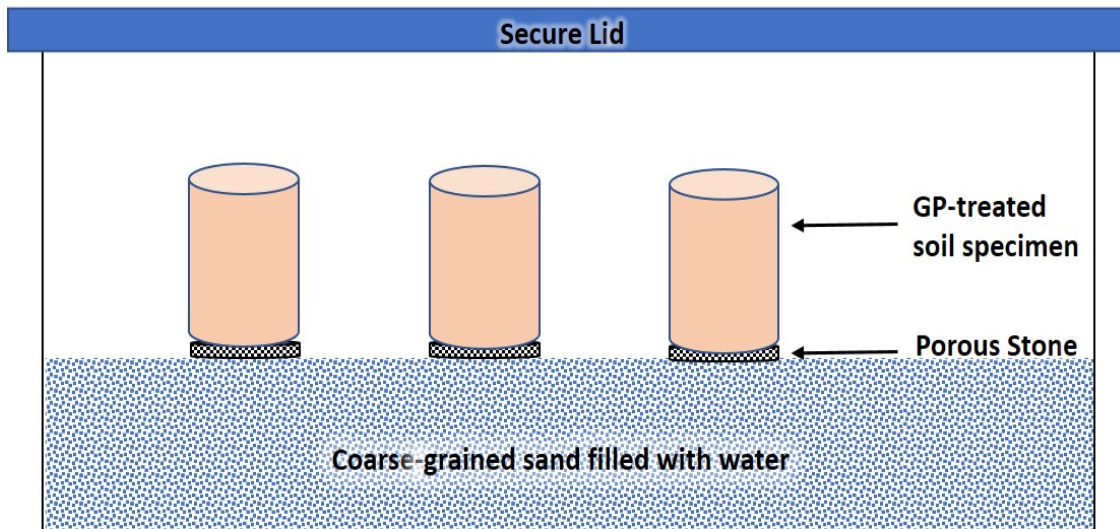

Figure 1. Durability setup by capillary soaking method.

After the prescribed days of curing, the GP-treated soil specimens are placed for capillary soaking for a period of 24 hours. The dimensions and mass of the soil sample are recorded just before and after the 24-hour period. After the capillary soaking period of 24 hours, the sample dimensions are recorded and then subjected to unconfined compressive strength testing.

4.5.2. Leachate Testing

In addition, leachate testing of geopolymer-treated samples was conducted as well using the setup as shown in Figure 2. This setup is a modified version of the one used by *(87, 88)*. Both CL and CH soil are treated with the lowest and highest (4% MK, 15% MK GP) geopolymer application ratios in this study, cured for 7 and 28 days before being subject to leachate testing. The compacted soil specimen was placed within a latex membrane and submerged in water with porous stones at the top and bottom of the setup under a hydrostatic pressure of 4 ft. of water. The leachate is collected through the outlet at the base after a period of five hours. The purpose of the leachate test is to determine the leachability of the specimen based on the volume of leachate discharge as well as to determine the concentration of source alkali (potassium) ions in the discharged leachate.

Figure 2. Leachate testing setup.

5. ANALYSIS AND FINDINGS

5.1. Properties of Pure GPC

Because GPC is often compared to the OPC. OPC samples were processed and characterized in the same conditions for the most accurate comparison. All the properties of the OPC samples are presented in Table 7 for later comparison with pure GPC.

Table 7. Summarized properties of OPC.

Property	Result
UCS at 14-day Curing	5923±865 psi (40.8±6.0 MPa)
Shrinkage	0.86±0.11%
Water Loss	29.58% to 28.67% to 21.25% (Week 0 to 2)
Density	1.58±0.04 g/cm^3
Open Porosity	5.46±0.70%

5.1.1. UCS of Pure GPC

For the UCS study of pure GPC and GPC/sand, the original framework was to follow ASTM C109 *(77)*, which requires the samples to be 2 in. cubes. The limited results include the UCS from 3 samples of Na331 and Na241 each and 1 sample of K241 (Figure 3). However, the testing was stopped at this point since the tests were approaching the limit of the load cell of the compression frame while the samples were expected to get even stronger as the test continues. Also, the values were lower than expected as the compositions were compared to the results from a previous study *(56)*, so the hypothesis was that the GP did not fully cure within 7 days. Therefore, the new set of samples was prepared by a more extensive 2-step 14-day procedure starting with curing under sealed condition for 7 days followed by curing in ambient condition for another 7 days.
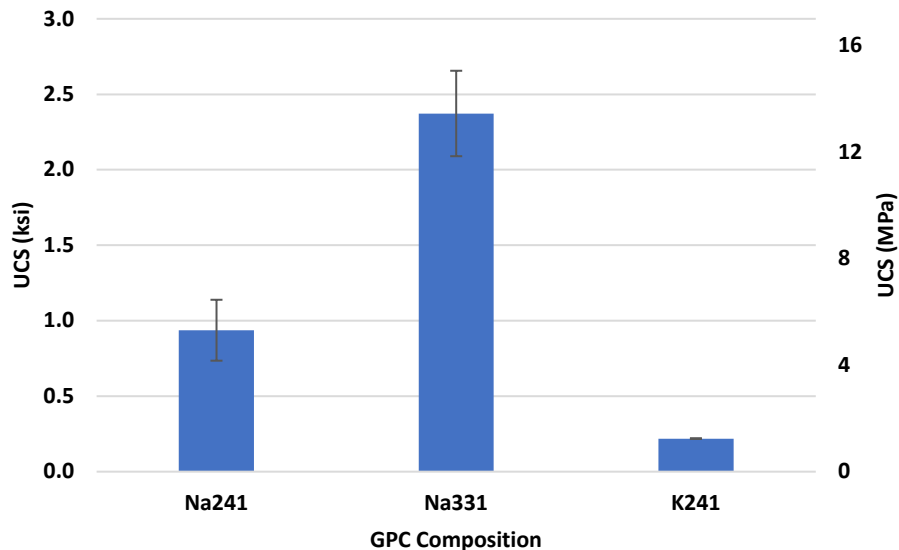

Figure 3. UCS of pure GPC at 7-day curing according to ASTM C109.

For a comprehensive parametric study of samples prepared using new curing conditions, it was necessary to test both Na-based and K-based GPC while ranging both the SiO_2/Al_2O_3 and H_2O/Solids ratios. Figure 4 shows preliminary compressive strength of pure GPC binder with 5

13

different compositions tested after the 2-step 14-days curing mentioned above. As expected, UCS increases with either decreasing water content in the GPC or increasing SiO_2/Al_2O_3 molar ratio. However, these samples were tested without measuring water loss, density, and porosity; therefore, the test was restarted to ensure that all the proposed tests and measurements are carried out with the same set of samples.
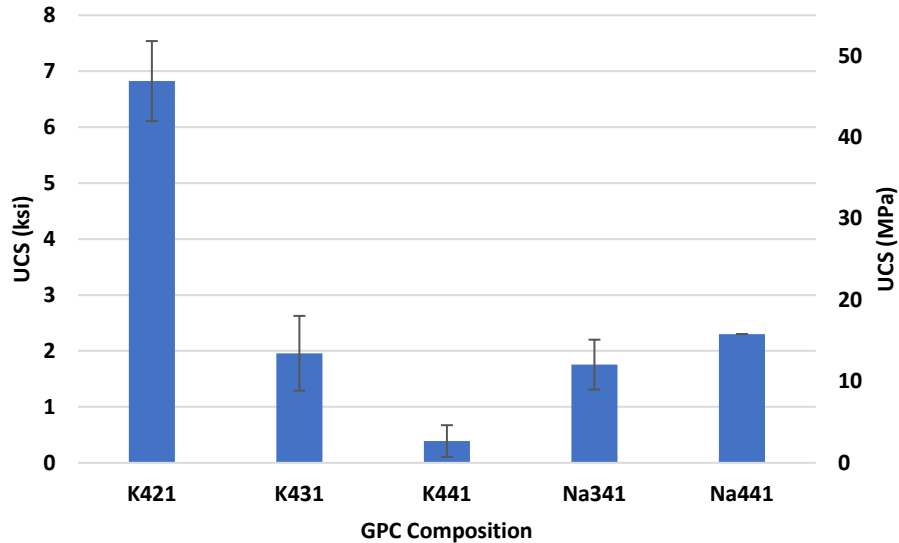

Figure 4. UCS of small GPC after 14-day curing.

Because of large variability in compressive strength between samples with different composition, this study extended the 16 sets of pure GPC binder sample with different composition after 14-day curing that also included density/porosity measurements. Figure 5 and Figure 6 show the UCS results of those samples. As expected, the UCS decreases with increasing water/solids ratio while all the other parameters are constant. Diving deeper into Figure 5, it can be noticed that Na321 is an anomaly composition that does not follow the trend of better strength with higher SiO_2/Al_2O_3 ratio and lower water/solids ratio (compared to Na(2.5)31 and Na331). If Na321 were to follow the trend, it should have UCS of roughly 3 ksi or 20 MPa. This is because Na321 GPC gels quickly during processing and only allows the shear mixing for ~100 seconds even at the lowest speed (100 RPM), while all the other compositions are mixed for 300 seconds at much higher speed. This means Na321 is most likely not mixed properly due to low workability (i.e. not enough water in the system), and most likely has clumps of unreacted MK, which leads to the poor strength. It's recommended that to fully optimize the strength for Na-based MK GPC, that compositions such as Na3(2.5)1, Na(3.5)21, and Na4(1.5)1 have to be explored in the future.

One of the downsides of using non-standardized sample dimension is that the numbers presented here only provide a qualitative understanding, and they might not necessarily be reproducible. Therefore, it will be helpful to remake some of the selected compositions into a standardized dimension (2 in. cube for ASTM 109), so that future studies can make valid quantitative comparison with our results. Looking at Na241 and Na331 in Figures 3 and 5, it can be seen that the average values match up well. However, the variation on smaller Na331 in Figure 5 is much larger than that in Figure 3, which could be an indication that small samples resulted in the high variation.
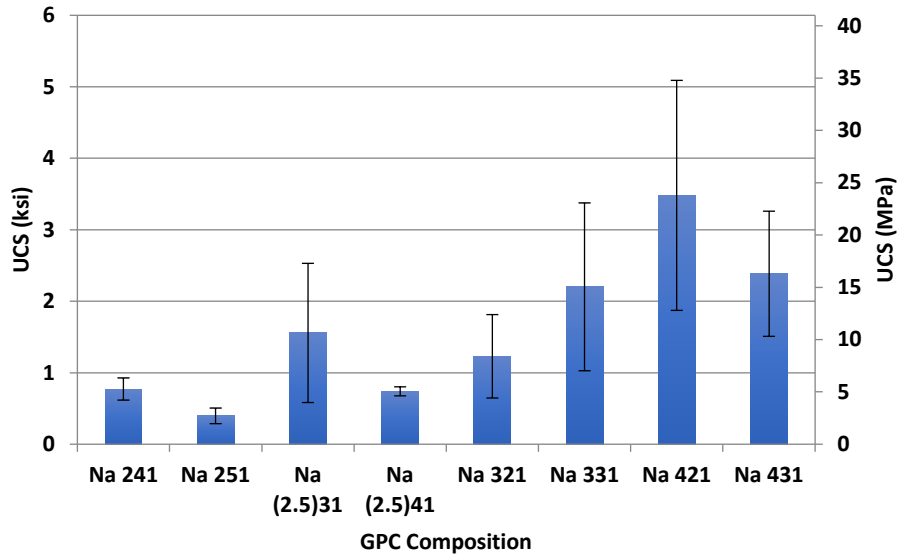
14

Figure 5. UCS of Na-based small GPC after 14-day curing.

As shown in Figure 6, K-based GPCs do not follow the hypothesized trend as the Na-based GPCs do for SiO_2/Al_2O_3 ratio. This could be due to the inherently slower geopolymerization kinetics between K-based GPCs and Na-based GPCs. Therefore, it would be interesting to revisit the composition after a longer period of curing (i.e. 28 days, or even 90 days) and then once again compare the strength. Since previous work *(89)* has demonstrated K-based MK GPCs cured at elevated temperature with better mechanical properties comparing to Na-based MK GPCs. For further optimizing the early strength of K-based GPC, it is worth investigating additional water reduction at higher SiO_2/Al_2O_3 ratio with compositions such as K3(2.5)1, Na(3.5)(1.5)1, and K4(1.25)1.

Comparing K421 and K431 values between Figures 4 and 6, the values differ drastically. The only significant difference in processing between these 2 sets of samples is that the K421 and K431 with lower values from Figure 6 were tested after density and porosity measurements. Since the samples were submerged in ethanol and had ethanol forced into the open porosity under vacuumed condition, it's possible that the process resulted in the formation of internal cracks for some composition. This can be easily tested by retesting some of the compositions without density/porosity measurements.
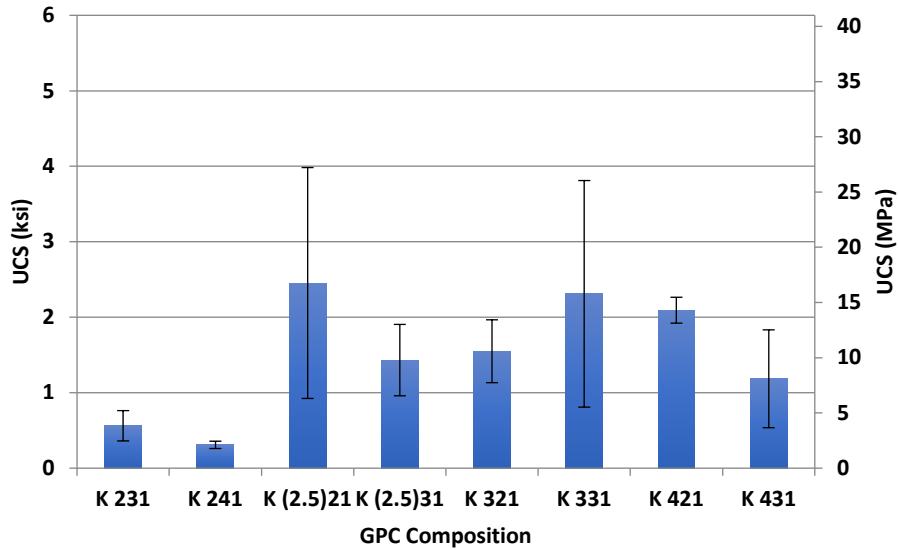
Figure 6. UCS of K-based small GPC after 14-day curing.

It's clear that OPC and GPCs cured at elevated temperatures *(47)* have better strength when compared to almost all the GPC compositions except for Na421 after 14-day curing at ambient conditions. However, GPC can still have significant strength development into the range of 20-35 MPa as it was showed in the previous study *(47)* when cured at elevated temperature for just 1-2 days. Therefore, it will be worth investigating the 28-day ambient-cured strength of GPC compositions with high SiO_2/Al_2O_3 ratio and low water/solids ratio, as well as investigate the proposed compositions above for further optimization.

5.1.2. Shrinkage and Water Loss of Pure GPC

As shown in Figure 7, most of the compositions shrink on average for only 0.55-0.65% during curing of 14 days, except for Na421, which is slightly higher, and Na241/Na251 which have low shrinkage. However, Na241/Na251 are weak and most likely have incomplete geopolymerization.
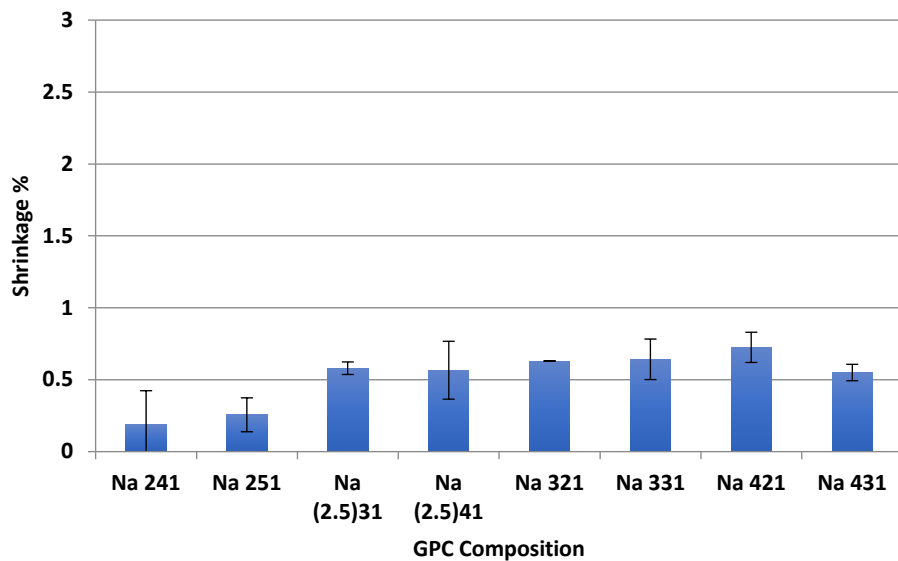

Figure 7. Shrinkage of Na-GPC.

16

Interestingly, K-based GPC shows a slightly different behavior. From Figure 8, most of the compositions shrink between 0.65% and 0.75% during curing. Samples with high SiO_2/Al_2O_3 ratio compositions (K421 and K431) have extremely high shrinkage values in comparison. When compared to OPC (Table 7), it's clear that all Na-based GPC have advantage over OPC, except Na421; the latter happens to have the highest UCS value. On the contrary, K-based GPC's shrinkage values are within the standard deviation of shrinkage measured in OPC during curing, with exception of K421 and K431, which shrinkage during curing is well above that of OPC.
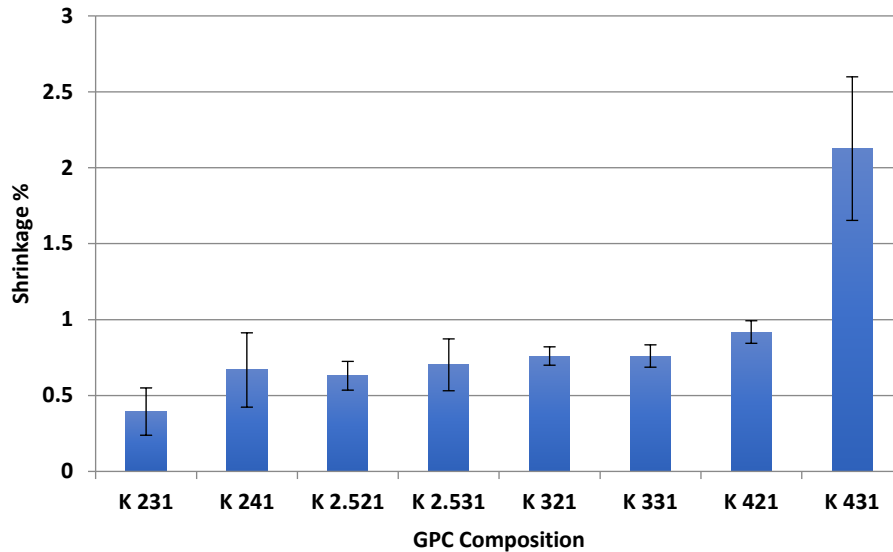
Figure 8. Shrinkage of K-GPC.

Water loss of Na-based GPCs during curing for 14 days determined from the mass changes of the samples and results are summarized in Figure 9. It is interesting to note that most of the compositions are around 20wt.% water after 2 weeks after mixing, similar to OPC (Table 7), regardless of their initial water content. With the exceptions of Na241 and Na421 which had very minimal water loss for the reason that are not clear at this moment.
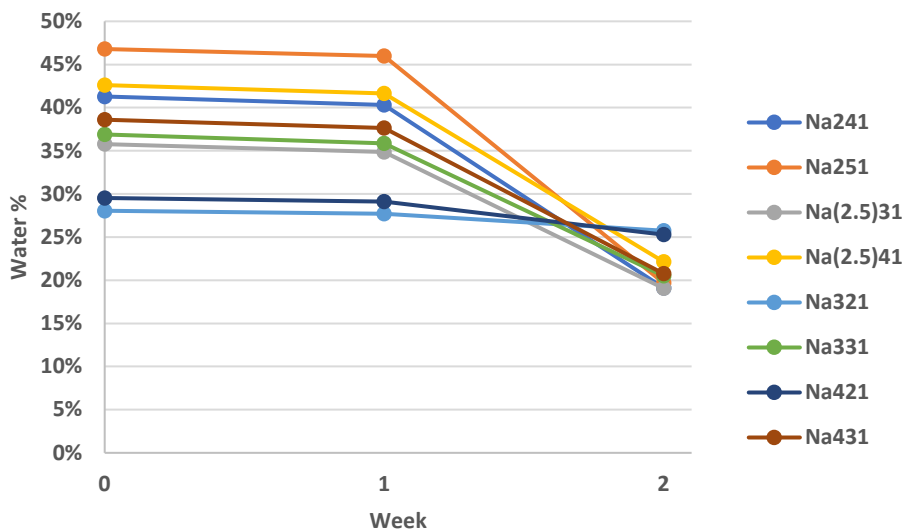
Figure 9. Water loss curve of Na-GPC.

On the contrary, since K-based GPCs have less initial water %, they also end up with less water in the system. The majority of the compositions contain ~10-15wt.% of water (see Figure 10). This difference in the water content between Na- and K-based GPC can account for higher shrinkage of the K-based GPC when compared to Na-based ones and OPC.
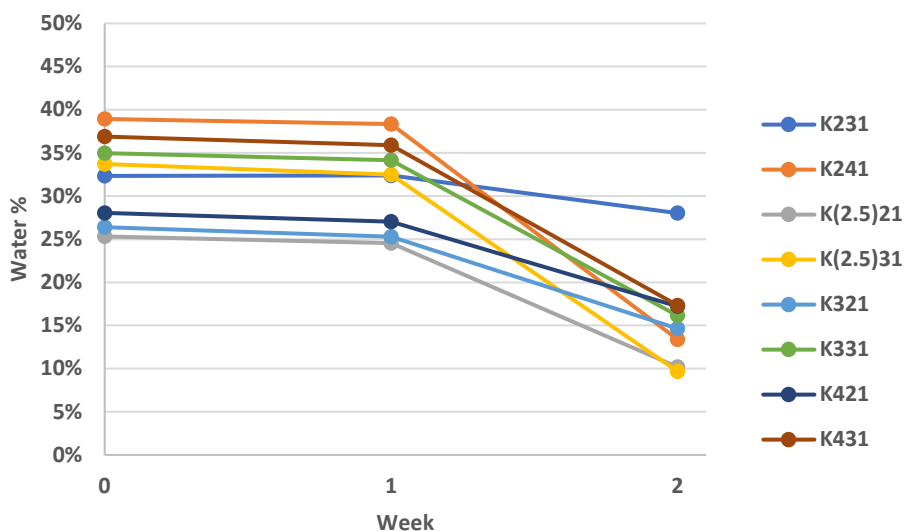
Figure 10. Water loss curve of K-GPC.

5.1.3. Density and Open Porosity of Pure GPC

Density and open porosity are properties that are closely related. If the bulk sample has low porosity, then it most likely has higher density, and vice versa. From Figure 11, all the GPC samples are plotted in relation to porosity and density. All but one outlier (this sample contained entrapped air bubbles) follows a clear trend. It can also be noted that all the points in the top left corner, i.e. low density and porosity samples, are GPC with low SiO_2/Al_2O_3 ratio and high water/solids ratio.
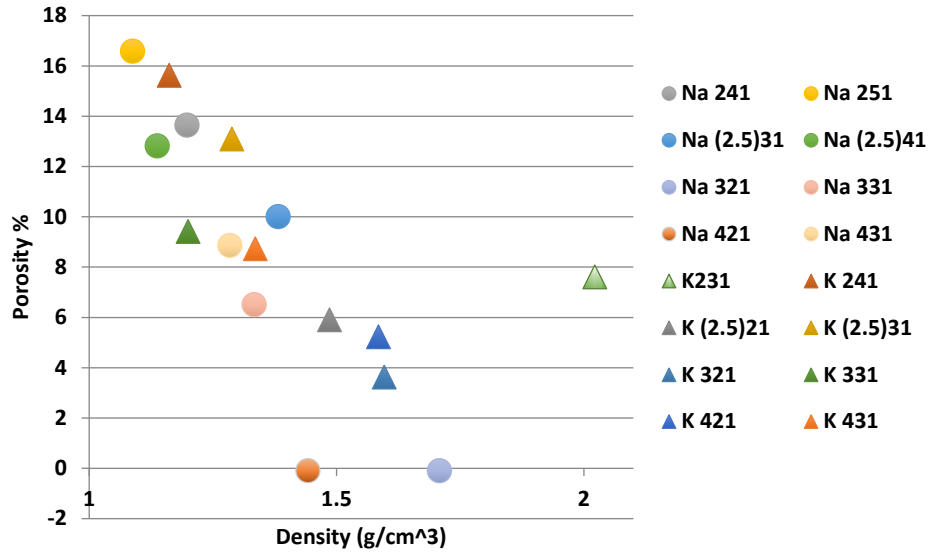
Figure 11. Porosity vs. density plot for pure GPC binder.

Conventionally, it's expected that higher density results in better mechanical properties for GPCs *(47)*. However, as Figure 12 shows, the UCS of the pure GPC binder samples peaked at ~1.5 g/cm³, and any samples with higher density exhibits drastic decrease in UCS. The two specific compositions are Na321 and K231, which coincidentally have been the outlier compositions in all the other properties. A possible explanation could be that these two compositions did not have enough water in the system for complete geopolymerization and sufficient workability, which then left large pores within the paste caused by entrapped air during mixing.
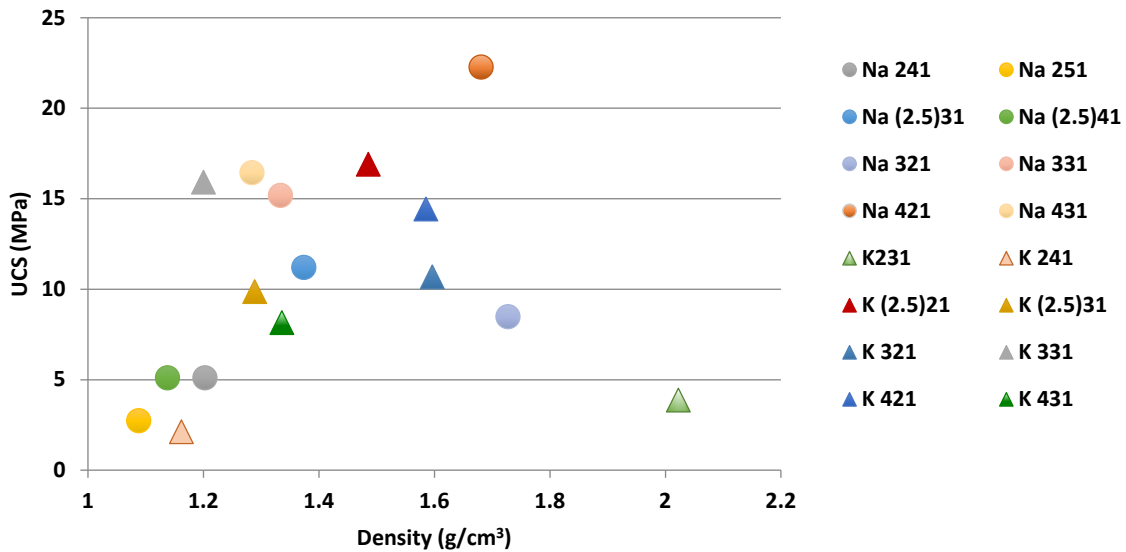
Figure 12. UCS vs. density plot of pure GPC binder.

5.2. Properties of GPC/Sand

5.2.1. UCS of GPC/Sand samples

Figure 13 shows UCS of GPC/sand samples (i.e. GPC mortar) with various amount of GPC (namely 8, 15, and 27wt.%) and various GPC compositions (namely K441, Na341, and Na441). Figure 13 clearly indicates that adding more GPC to GPC/sand mixture leads to significant increase in compressive strength. At 8% GPC, the UCS does not vary significantly among samples with different GPC compositions; however, at 27% GPC, the effect of composition becomes more significant. The size of the error bars increases significantly as UCS increases. This could indicate that a larger samples size is needed to obtain more statistically representative results according to Weibull distribution *(90)* and recommendations in the literature *(91)*.
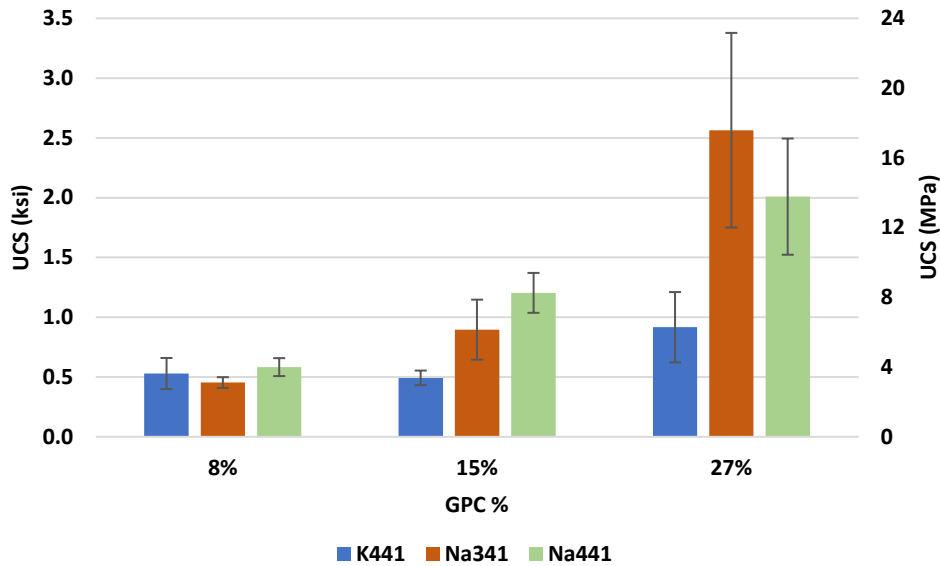
Figure 13. UCS of small GPC/sand at various % after 14-day curing.

For further compositional study, GPC/sand samples with 27wt.% of GPC of various compositions (total of 8 different GPC compositions for both Na and K activated GPCs) were processed and tested in compression after curing for 14 days. Results in Figure 14 for Na-based GPC/sand samples show higher UCS values, when compared to pure GPC (Figure 5). However, values only follow the expected trend for the lower SiO_2/Al_2O_3 ratio. Once SiO_2/Al_2O_3 ratio is above 3, the UCS seems to saturate and even show some decrease for Na421, which is the pure GPC composition with the highest strength in this study. One possible explanation for this behavior is the alkali-aggregate reaction: since Na421 activator has a higher pH, it can easily lead to solution of SiO_2 from the surface of the sand particles into the system and increase the SiO_2/Al_2O_3 ratio in the GPC binder. As Lizcano pointed out in her work *(56)*, SiO_2/Al_2O_3 ratio > 4 greatly decreases the UCS. Another composition with interesting behavior is Na321, which was pointed out to be the anomaly composition; however, when sand is added, the additional mixing most likely allowed the system to geopolymerize fully. In addition, alkali-aggregate reaction most likely occurred in this system, but in this case, it actually helps make the system more workable (easier diffusion and transport of units) resulting in a higher UCS.
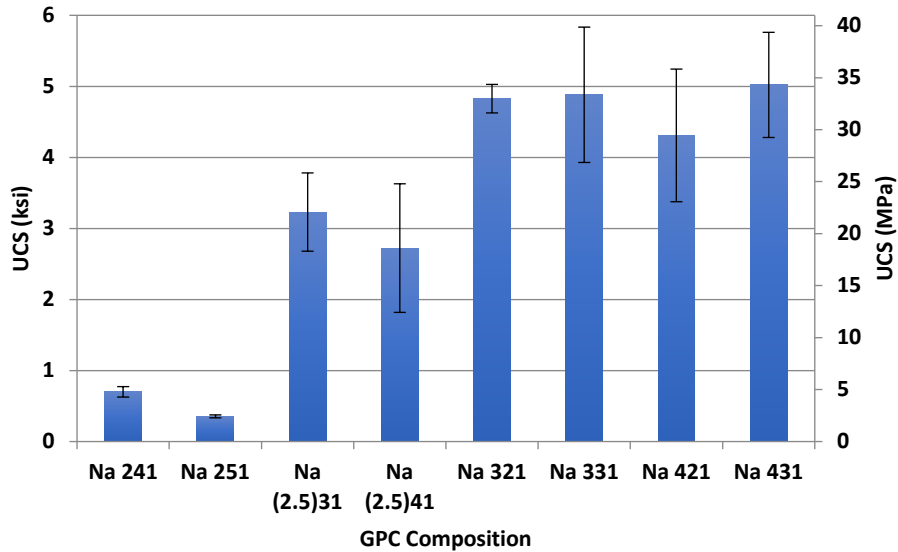
Figure 14. UCS of small 27% Na-GPC mortar at 14-day curing.

From Figure 15, it can be seen that the UCS value of K-based GPC/sand samples also increased significantly when compared to pure K-based GPC (Figure 6) by addition of 27wt% of sand to the system.
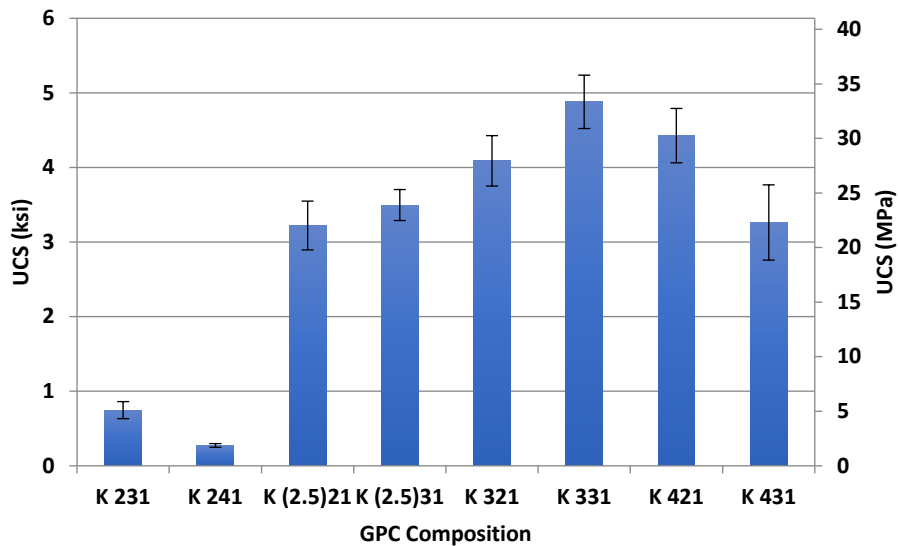
Figure 15. UCS of small 27% K-GPC mortar at 14-day curing.

5.2.2. Shrinkage and Water Loss of GPC/Sand

Across the board, the shrinkage of GPC/sand during the 14-day curing at the ambient temperature decreased with the addition of sand, when compared to the pure GPC. This observation is valid for both Na-based (Figure 16) and K-based (Figure 17) GPC/sand samples. The large error bars observed in both figures below are most likely from the combination of small sample size (25.4 mm), low shrinkage values, and measurement tool resolution (caliper with 0.01 mm resolution).
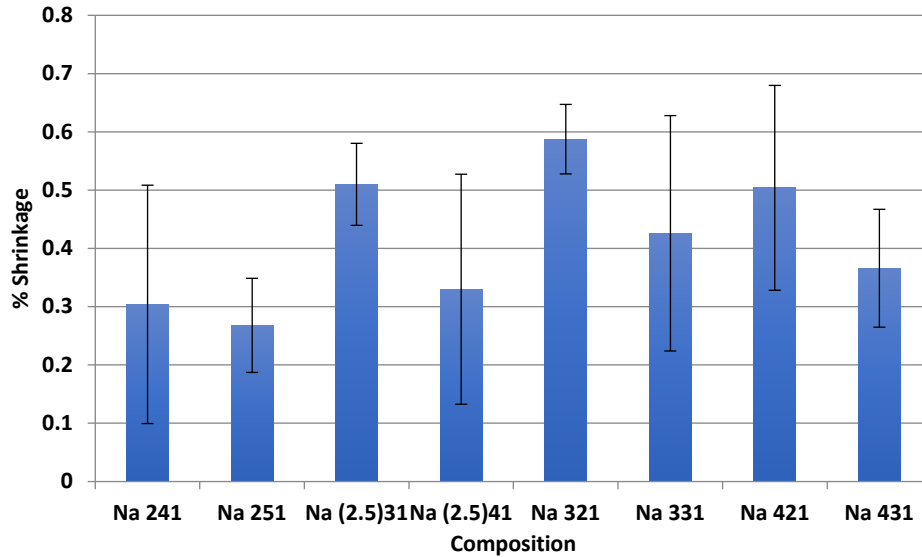
Figure 16. Shrinkage of 27% Na-GPC/Sand.
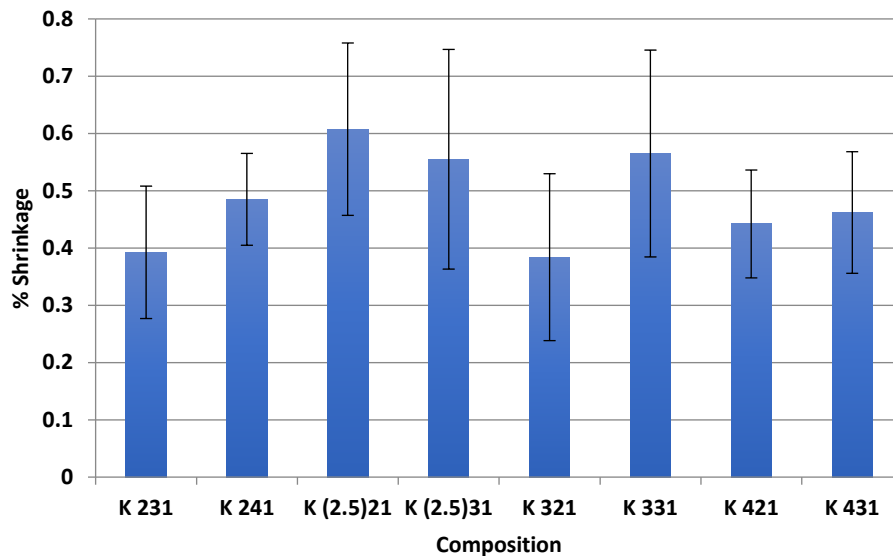
Figure 17. Shrinkage of 27% K-GPC/Sand.

Water loss data for GPC mortar is not presented here, since the trend is very similar to pure GPC binder but at a smaller percentage of the overall sample.

5.2.3. Density and Open Porosity of GPC/Sand

Unlike the clear trend with pure GPC binder, Figure 18 does not show a clear trend initially. However, with a closer investigation of the Na-based GPC mortar (circle) points, it can be observed that they follow the expected downward (increasing density results in lower porosity). Although the K-based GPC mortar (triangle) have 5 points with a clear trend, the other 3 points are scattered. This could be due to processing of GPC mortar samples; if not well-packed, can lead to variance.
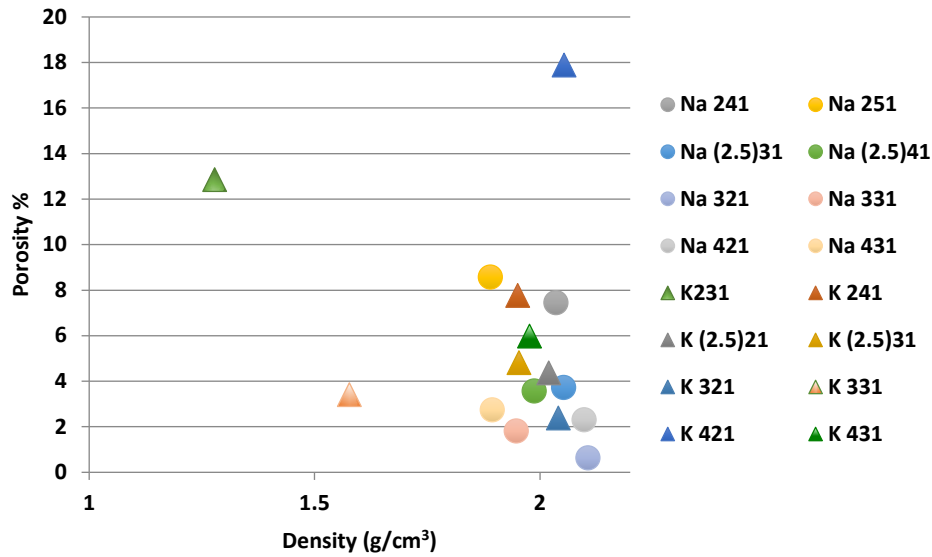
Figure 18. Porosity vs. density plot of 27% GPC mortar.

Similarly, Figure 19 does not exhibit a clear trend. Most likely due to a similar reason as above, where the GPC mortar samples contain a small amount of GPC. Another factor could be poor processing during sample fabrication.
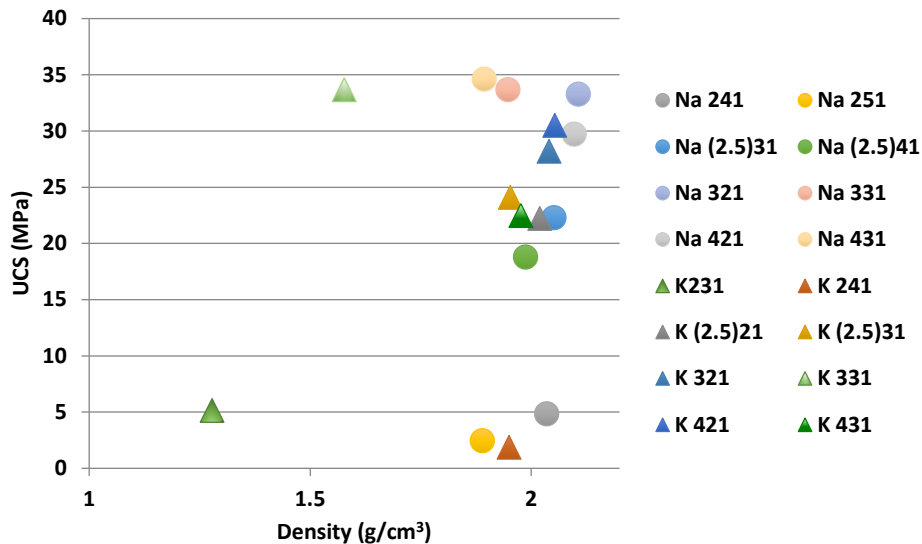
Figure 19. UCS vs. density plot of 27% GPC mortar.

5.3. SEM of GPC/Sand

To fully understand the behavior between the aggregate (sand) and GPC, it is important to investigate the morphology at the interface of the 2 phases. Selected and typical SEM images, GPC, sand, and GPC/sand samples are shown in Figure 20 GPC has a nanoporous morphology as expected from previous published results *(92)*.
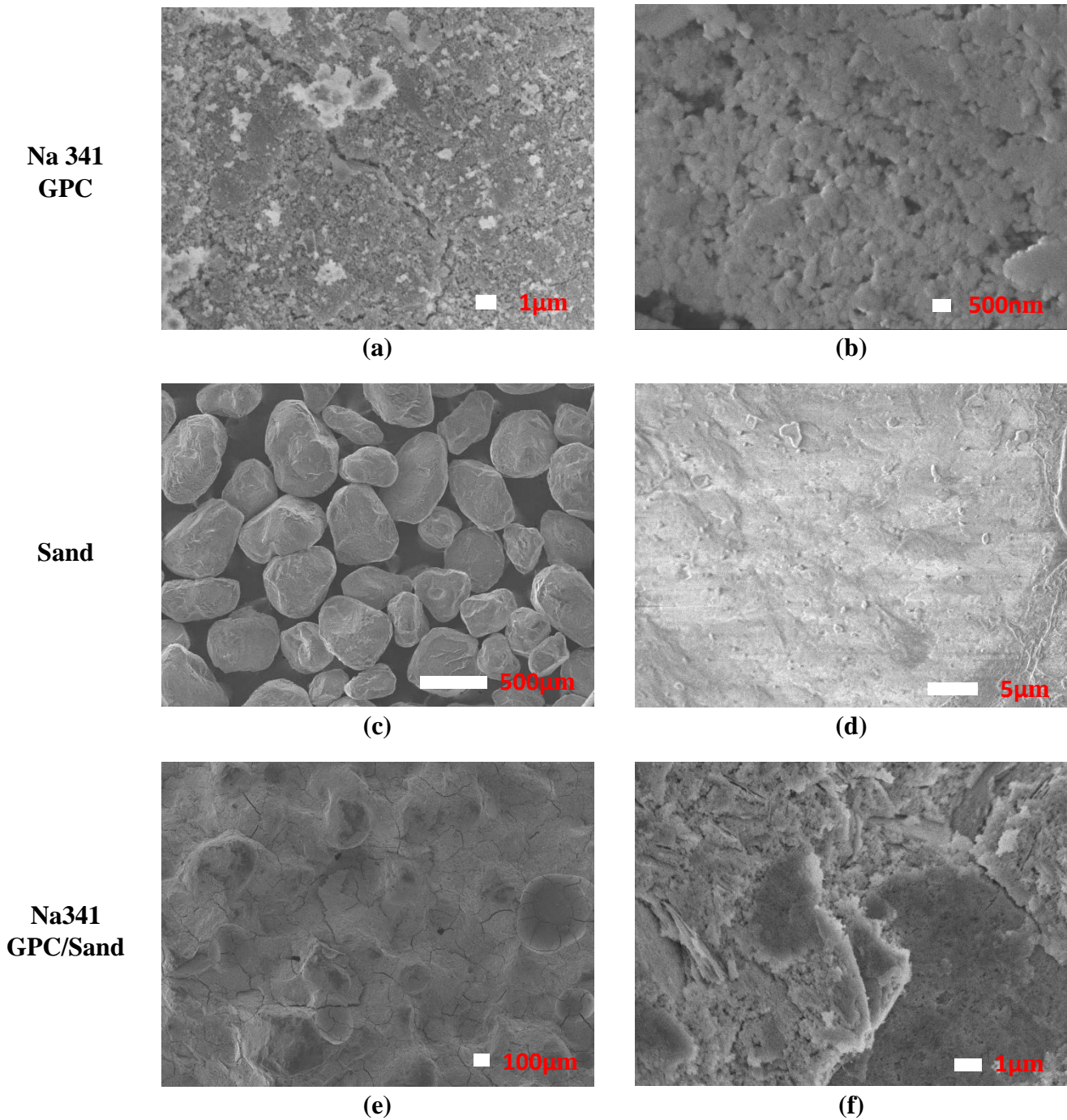
Figure 20. SEM micrograph of GPC in: (a) Low Magnification - 5.5kX, (b) High Magnification - 27kX; Sand in (c) Low Magnification - 37X, (d) High Magnification - 2.7kX; GPC mortar in (e) Low Magnification - 40X, (f) High Magnification - 7.5kX

On the contrary, sand particles have a dense morphology, and the average size is on the order of 100 μm. As shown, we cannot observe the interface of the GPC mortar due to the apparent good adhesion between GPC and sand. In order to observe the interface morphology between the two phases, it will be necessary to use high-precision sectioning instruments such as a high-speed saw to view a clean cross-section of the GPC/sand specimen. From there, another SEM can be

performed and possibly in situ mechanical testing, such as micro/nano indentation to understand the adhesion behavior quantitatively.

5.4. Parametric Study of UCS in GP-CL System

From the effect of %MK in Figure 21, it agrees with the results on K431 that there's a significant increase when increasing the dosage above 4%; however, increasing from 7.5% to 10% resulted in a small decrease. This could be due a low H_2O%, resulting in the GP not having enough H_2O to fully geopolymerize.
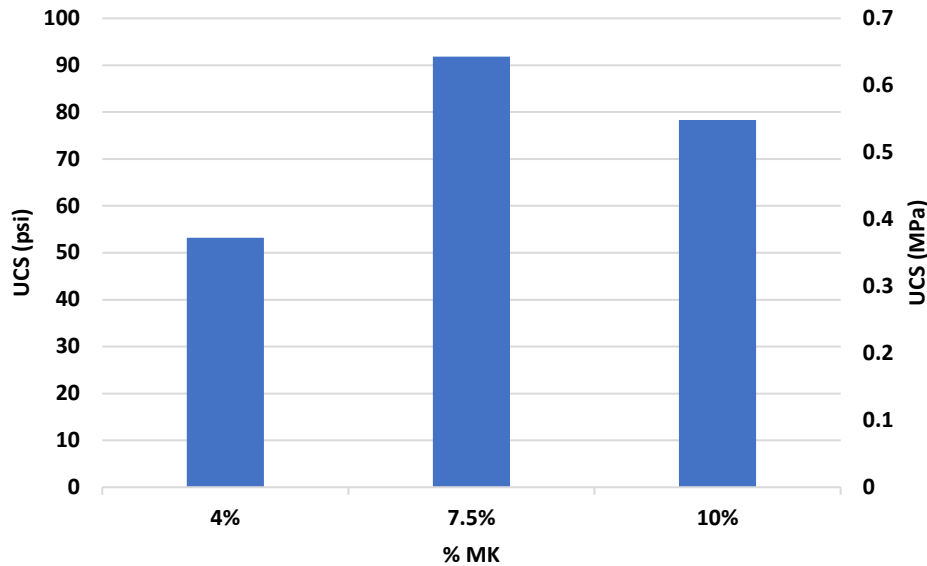
Figure 21. UCS trend with varying %MK from K421 at 7-day curing.

For the SiO_2/Al_2O_3 ratio test in Figure 22, the sample set are all using 4% MK with K421 GP while keeping the H_2O/Al_2O_3 ratio constant at 10. Keeping this ratio constant will result in similar viscosity, according to Lizcano et al. *(4)*. As expected with all the other literature findings, SiO_2/Al_2O_3 ratio is most optimal around 3.5 to 4, since the UCS from the 2 values are do not have any statistical significance. However, for the sake of the study, SiO_2/Al_2O_3 equal to 4 is concluded to be the most optimal value and used to further in the study.
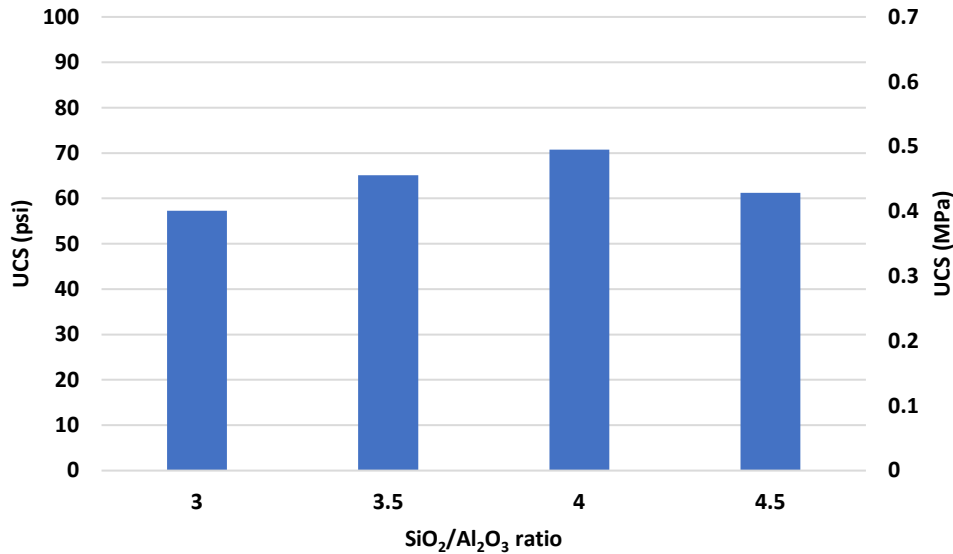
Figure 22. Effect of SiO₂/Al₂O₃ ratio at 4% MK and H₂O/A₂O₃=10 on UCS.

The effect of H_2O/Solids ratio for GP is not easy to predict, since it dictates viscosity, workability, and porosity significantly. For example, if the ratio is too low, then the GP will not mix well with the soil; on the other hand, if the ratio is too high, the resulted GP will be porous and weak. From Figure 23, it is shown that the optimal H_2O/Solids ratio is 3 for the K4_1 composition.

Figure 23 shows the effect on strength when GP-soil is dried. As expected, the strength increases; however, K431 did not exhibit the expected behavior. This is likely an anomaly and needs to be repeated to obtain results that are more statistically representative.
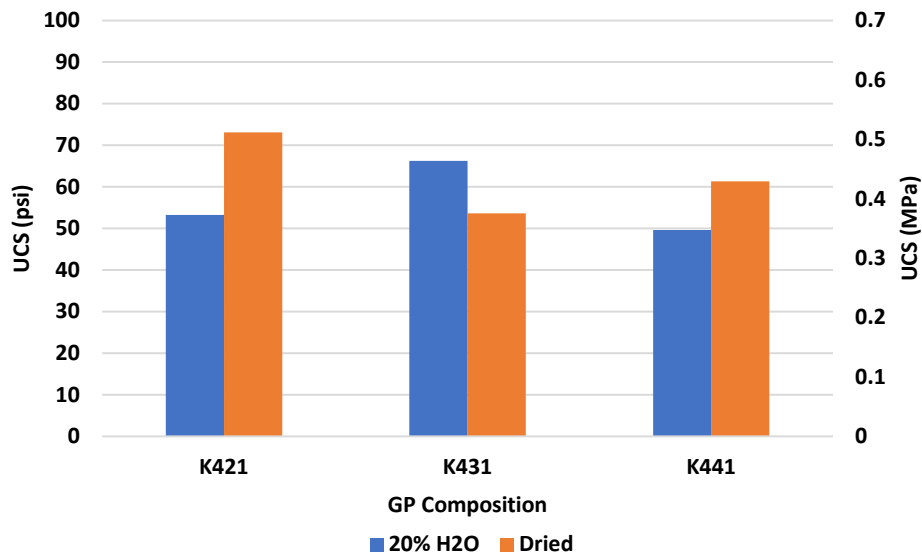
Figure 23. Effect of H₂O/Solids ratio and drying with 4% MK + CL at 7-day curing.

Continuing the testing with K431, Figure 24 demonstrates the parabolic behavior with total H_2O% and the significant increase in strength upon drying (except at 20% which is an anomaly as mentioned above). The effect of total H_2O% is expected: there is a change in maximum dry density

26

with the change of $H_2O\%$. Therefore, UCS in relation to the total $H_2O\%$ exhibits a similar behavior, and in the case of 4% MK K431 + CL, 20% H_2O seems to be the closest to the optimal. Interestingly, it appears that dried samples exhibit roughly the same UCS value no matter what the UCS percentage while wet. This could mean that the total $H_2O\%$ does not matter during the process and that geopolymerization happens as long as the sample dries.
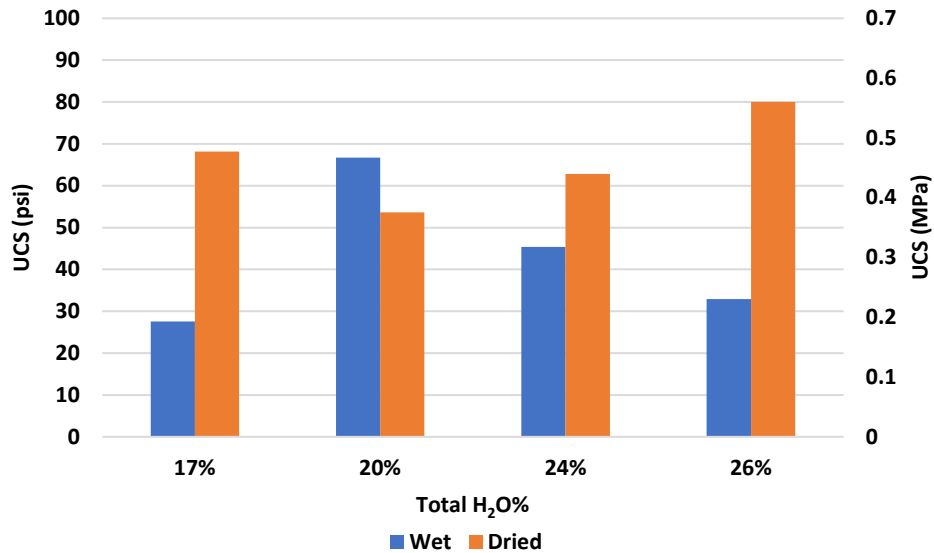
Figure 24. Effect of total $H_2O\%$ on UCS with 4% MK K431 + CL at 7-day curing.

5.5. UCS of GP-Treated Soil

The UCS of K431 geopolymer-treated soil samples cured in 100% RH for a period of 0, 7, and 28 days were tested. These tests were conducted at a strain rate of 0.03 in/min, so as to negate the influence of the shearing rate on the peak stress *(25, 93)*. Figure 25 shows the UCS of geopolymer-treated CL at the ratio of 4%, 10%, and 15% Metakaolin in geopolymer to dry soil. All UCS samples were compacted at 95% of their respective MDDs and OMCs. The untreated CL specimen shows a UCS value of 15 psi, while the 4% MK geopolymer treated CL specimens have a UCS of 44 psi after 28 days of curing, which is about a 190% increase in its UCS value compared to the untreated CL. The 10% and 15% MK geopolymer-treated CL also show significant increase in UCS in the range of 350-750%. It is observed that for the lower geopolymer treatment (4% MK GP), strength increase is almost immediate, while for the higher geopolymer treatments, the highest UCS is observed to be on the 28th day of curing.
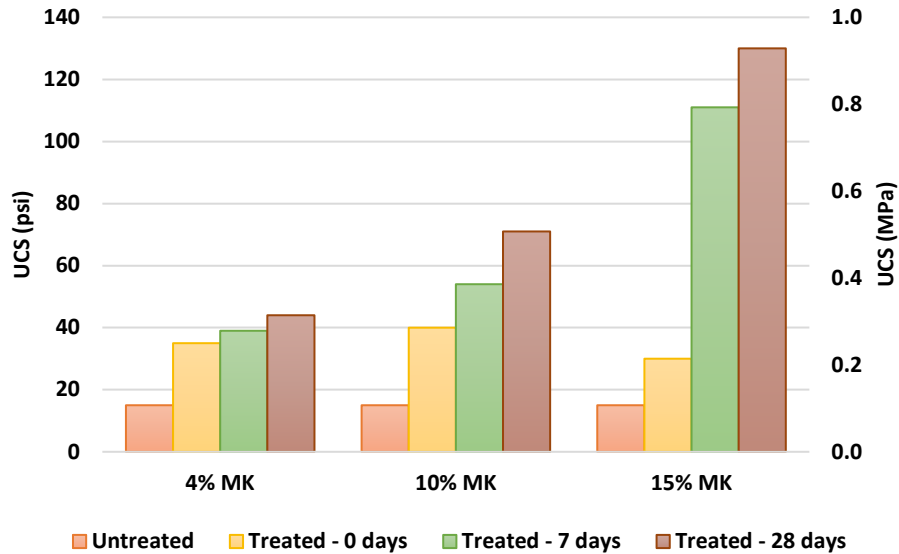
Figure 25. UCS of geopolymer-treated CL soil.

Similarly, UCS of geopolymer-treated CH is shown in Figure 26. The untreated CH shows a UCS value of 20 psi, while the 4% MK geopolymer-treated CH has a UCS of 40 psi after 28 days of curing, which is a 100% increase in its UCS value compared to the untreated CH. The 10% and 15% MK geopolymer-treated CH also show significant increases in UCS in the range of 200-500%. As observed in geopolymer-treated CL, strength increase in the lower geopolymer treatment (4% MK GP) is almost immediate, while for the higher geopolymer treatments, the highest UCS is observed to be on the 28th day of curing. On comparing both soil types, CL is observed to have much higher UCS values for the higher percentages of geopolymer application (10% MK, 15% MK) than CH for those sample application ratios of the same geopolymer. Note that for 15% MK geopolymer-treatment of both soils, significant strength increase is not attained until day 7 of curing.
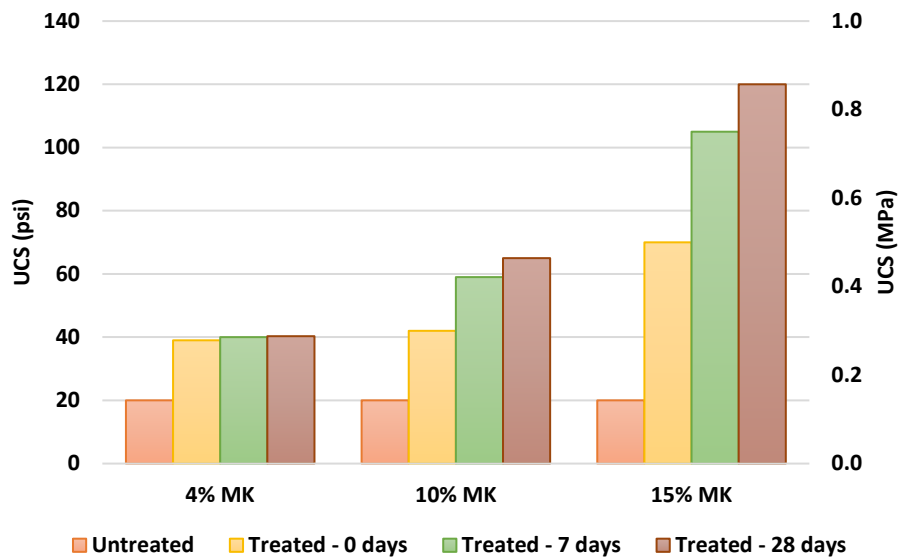
Figure 26. UCS of geopolymer-treated CH soil.

5.6. pH of GP-Treated Soil

Geopolymer-treated soils were tested for pH after a curing period of 0, 7, 14, 21, and 28 days. Conventionally, the lowest percentage of lime required to stabilize a soil is 12.4, which is the pH of a saturated lime solution. Elevated pH levels are known to significantly boost the dissolution of silica and alumina in clay, thus enabling them to interact with available cations. The subsequent consumption of the cations from the reactive solution releases H+ ions into the solution resulting in a decrease in pH. As such, it is important to establish that a high-alkaline environment is provided for the initiation of required physico-chemical reactions. In addition, it is essential to determine that the pH does not drop drastically before the appropriate curing time to ensure enough reaction time. Figure 27 and Figure 28 shows the variation in pH for GP-treated CL and CH respectively for different curing periods. The lime-cutoff pH of 12.4 is also shown in the plots for comparison.
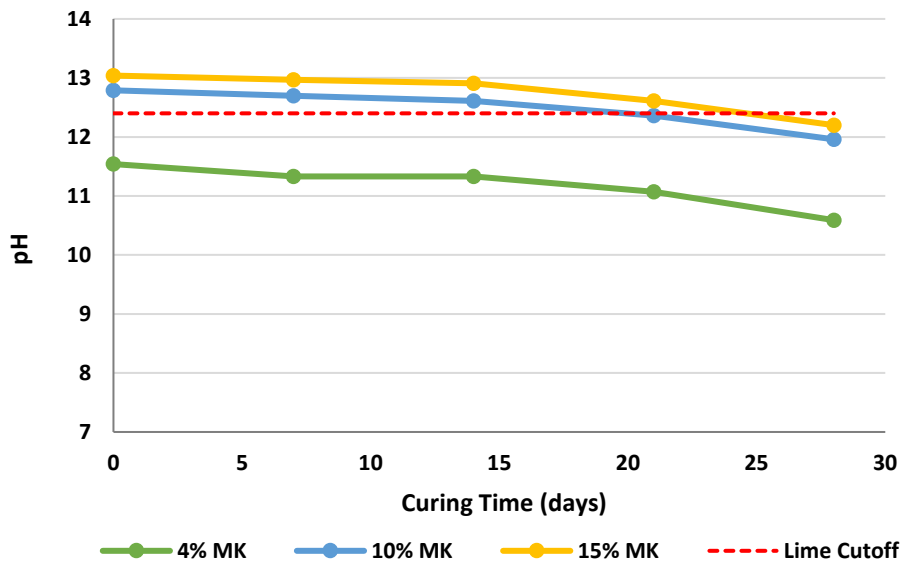
Figure 27. Variation of pH with curing time for geopolymer treated CL.

From Figure 27, we observe that the higher application ratios (10% and 15% MK-GP) have pH around 13 at 0 and 7 days, while the 4% MK-GP has a lower starting pH of around 11.5. An overall 6-8% decrease in pH is observed for all GP application ratios after 28 days. It is important to note that pH is observed to be below the lime-cutoff of 12.4 after 28 days.
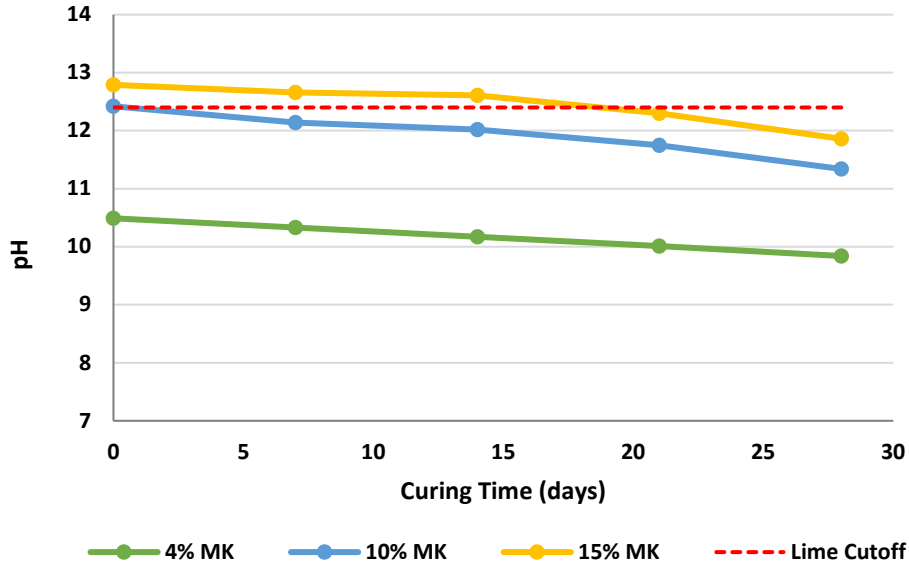
Figure 28. Variation of pH with curing time for geopolymer treated CH.

From Figure 28, we observe that overall pH of GP-treated CH is slightly lower as compared with GP-treated CL. The higher application ratios (10% and 15% MK-GP) have pH around 12.5 at 0 and 7 days, while the 4% MK-GP has a lower starting pH of around 10.5. An overall 6-8.5% decrease in pH is observed for all GP application ratios after 28 days.

5.7. Effects of Capillary Soaking on GP-treated Soil

Durability testing using 24-hour capillary soaking of geopolymer-treated soil samples was conducted. The structural characterization of GP-stabilized soils that underwent durability testing are shown below in plots detailing changes in UCS after curing periods of 0, 3, 7, 14, and 28 days. Figure 29 shows the UCS of geopolymer-treated CL and CH after capillary soaking.
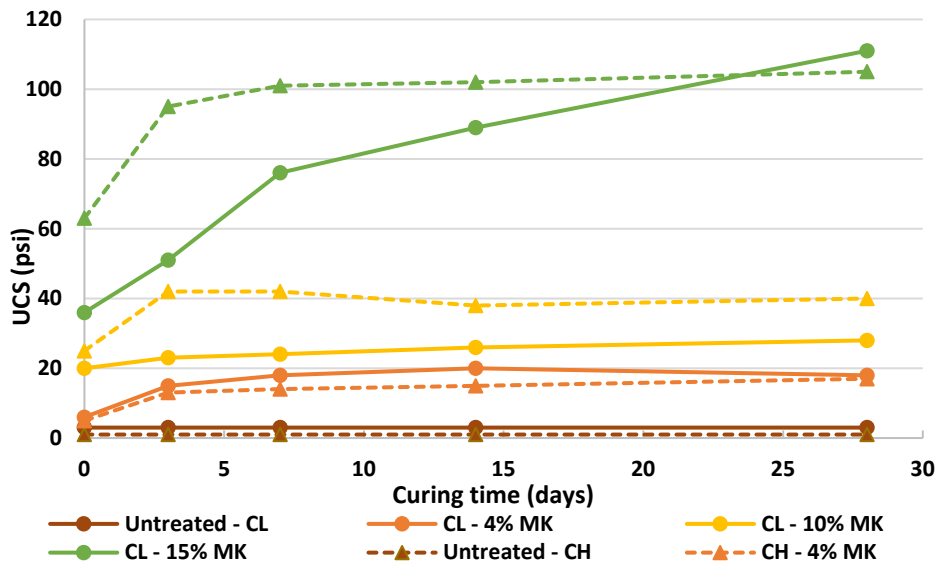
Figure 29. UCS of geopolymer-treated soils after durability testing.

From the above plot, we see that untreated soils have significantly low UCS (of 3 psi or lower) after durability testing. Geopolymer treatment of both soils shows significantly higher UCS values as compared to untreated soils. As expected, the higher the geopolymer application ratio, the higher the UCS value. The 4% MK geopolymer-treated soils both have a UCS of around 20 psi after 28 days of curing and are also observed to show a similar strength increase pattern. The 10% MK geopolymer-treated CL and CH show UCS of around 30 psi and 40 psi respectively, after 28 days of curing. CL is found to have lower UCS value than CH when treated with 10% MK geopolymer. On the other hand, 15% MK geopolymer-treated CL has slightly higher UCS than CH for the same application ratio. It is interesting to note that there is a difference of 30 psi in the 0-day UCS value of 15% MK geopolymer-treated CL and CH, and then CL exponentially increases to obtain a higher psi than CH at 28 days. Compared to the untreated soils subjected to durability testing, geopolymer-treated CL and CH subjected to the same durability treatment show momentous increase in UCS after final curing: in the order of 450-3,600% and 1600-10,400%, respectively.

Figure 30 and Figure 31 below show a comparison plot of UCS values for CL and CH respectively, with and without durability testing. Note that the bars with black-dotted borders indicate the UCS values after durability testing.
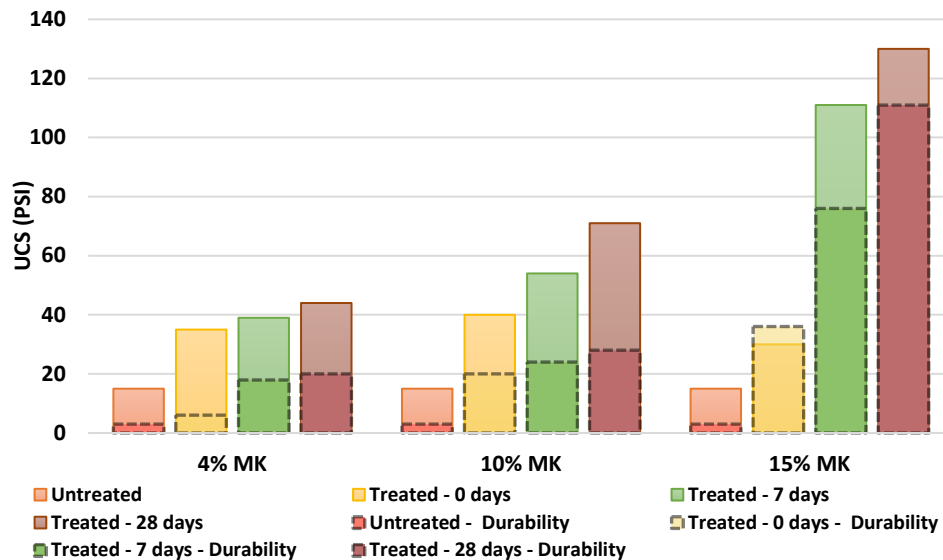
Figure 30. UCS comparison of geopolymer-treated CL with and without durability testing.

From Figure 30, there is a reduction in UCS values for CL specimens after being subjected to durability testing. As expected, the reduction in UCS values is significant for untreated CL. Higher GP application ratios show lower reduction in UCS values as compared to those CL specimens not subjected durability testing. The final percent decrease in UCS values of 4%MK, 10%MK, and 15%MK GP-treated CL specimen subjected to durability testing is about 55%, 60% and, 15% respectively. A curing period of 28 days is observed to provide peak strength for all GP application ratios. The 28-day curing period is found to be most crucial for the highest GP application ratio (15% MK GP), while a 7-day curing period results in UCS values similar to those from a 28-day curing period for both the lower GP application ratios (4% and 10% MK GP).
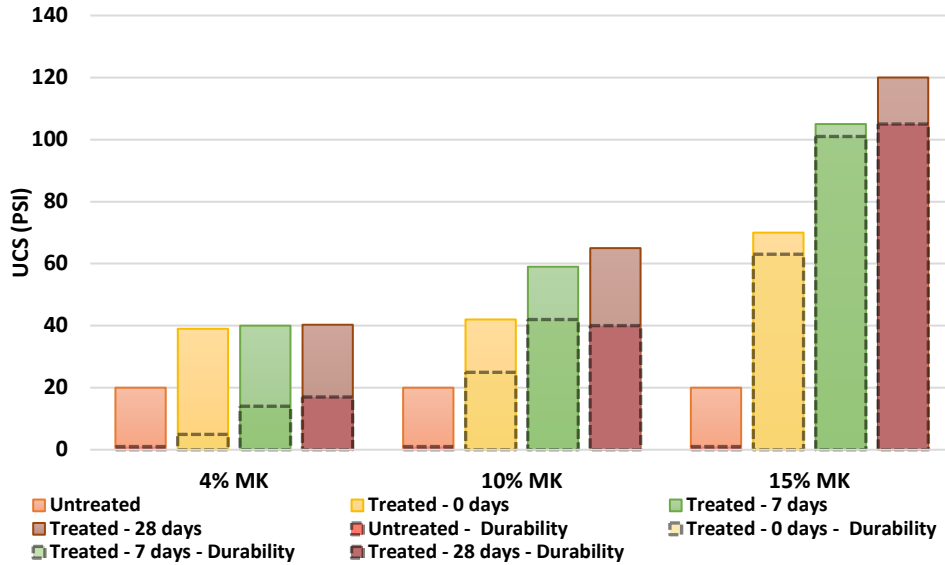
Figure 31. UCS comparison of geopolymer-treated CH with and without durability testing.

Similar to the trend n CL, there is reduction in UCS values for CH specimens (Figure 31) as well. As expected, the reduction in UCS values after durability testing is significant for untreated CH. Higher GP application ratios show significantly lower reduction in UCS values as compared to those CH specimens not subjected to durability testing. The final percent decrease in UCS values of 4%MK, 10%MK, and 15%MK GP-treated CH specimens subjected to durability testing is 57%, 3%, and 12%, respectively. Unlike what was observed in CL, a 7-day curing period is found to be sufficient for all GP application ratios, as a 28-day curing period does not result in significantly higher UCS values for CH specimen subjected to durability testing. From Figure 30 and Figure 31, it is observed that the reduction in UCS of untreated CL and CH subjected to durability testing is in the range of 80% and 95% respectively, when compared to untreated soils that did not undergo durability testing.
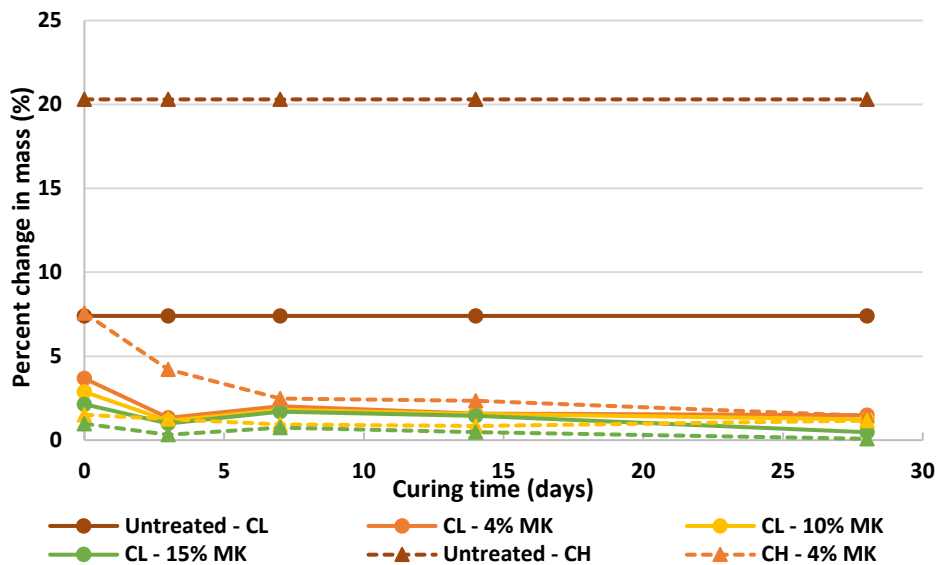
Figure 32. Percent change in mass of geopolymer-treated soils after durability testing.

From Figure 32, we see that untreated CL and CH is observed to have roughly 7% and 20% increase in mass, respectively, due to 24-hour capillary soaking. It is observed that GP-treatment of soils reduces their capacity for water intake and total mass increase is observed to be under 2% for both GP-treated CL and CH. While immediate decrease of water intake is noted at 0 days, curing time of 7 days is found to be sufficient in reducing water intake. Note that 4% MK GP-treatment on CH takes about 7 days for effective decrease in water intake unlike other treated specimens which have an immediate decrease. The highest application ratio of 15% MK-GP is observed to have the lowest percent change in mass for both treated CL and CH.
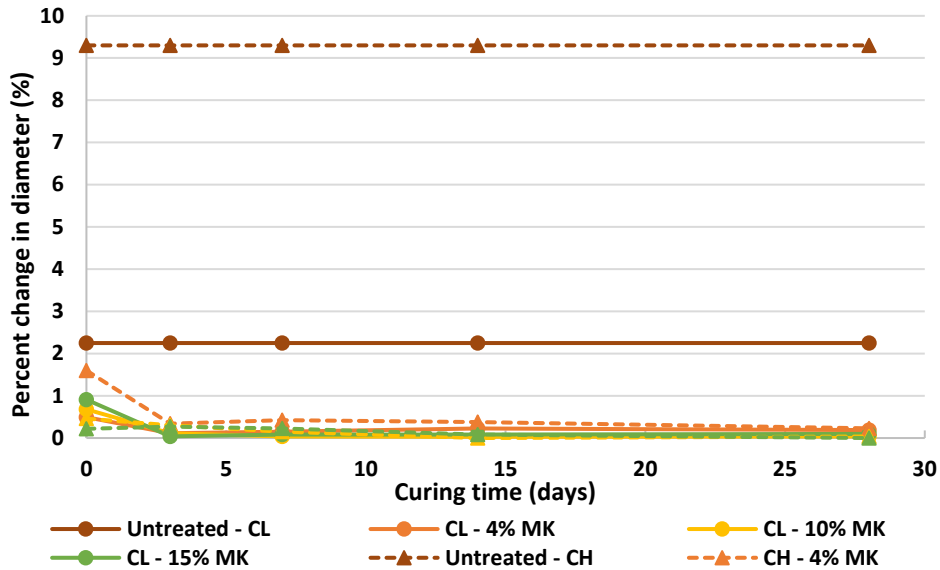
Figure 33. Percent change in diameter of geopolymer-treated soils after durability testing.

From Figure 33, untreated CL and CH is observed to have roughly 2% and 9% increase in diameter, respectively, due to 24-hour capillary soaking. Total diameter increase is observed to be under 0.5% for both GP-treated CL and CH. A curing time of 7 days is found to be sufficient in reducing diameter increase. It is observed that increased percent application ratios of GP, decreases the percent change in mass and diameter by decreasing its ability to draw water. 4% MK-GP application is observed to be sufficient to significantly reduce mass change and diameter increase in both treated CL and CH. Overall, geopolymer-treated soils are observed to significantly reduce the ability of soil to draw water as compared to untreated soils.

5.8. Leachate Analysis of GP-Treated Soil

Leachate testing was conducted on both soil types with the lowest and highest (4%, 15% MK) GP-treatment applications after 7 and 28 days. Leachate was collected for a period of 5 hours to observe the rate at which the leachate was discharged. All leachate collected was tested for potassium ion concentration. Results of the leachate test are presented in Table 8. While it is difficult to recognize a distinct trend between the volume of leachate and geopolymer treatment, increasing dosages of geopolymer treatments larger curing periods are mostly observed to lower the volume of leachate produced. An anomalous spike in leachate is observed for GP-treated CL and CH at 7 and 28 days respectively. Overall, GP-treated CL soil was observed to produce less leachate that GP-treated CH. It is possible that the lower amounts of leachate produced correspond to specimens where the soil bonded well with the geopolymer, resulting in less voids and therefore

less pathways for water to leach through. Untreated CL and CH soils were found to have 24 and 18 ppm of K^+ in their respective leachates. K^+ ion concentration was observed to be under 22,000 ppm for both soils after 4% MK GP treatment, while it escalated exponentially in the 15% MK GP-treated leachate of both soils, especially after a curing period of 7 days. GP-treated CH was observed to have much lower K^+ ion concentration was observed to be much lower for GP treated CH than for GP treated CL soils. It could be concluded that as curing time increases the concentration of K^+ ions decreases due to lesser availability of K^+ ions with reaction with clay minerals.

Table 8. Summary of Leachate test: Leachate volume and K^+ ion concentration in leachate.

Soil Type	GP Treatment	Curing Time (days)	Sample Mass (g)	Leachate per hour (ml)	K^+ ion (ppm)
CL	0%	0	1173	19	24
CL	4% MK	7	1120	14	22,000
CL	4% MK	28	1119	20	19,000
CL	15% MK	7	1195	42	165,000
CL	15% MK	28	1198	13	117,500
CH	0%	0	1108	32	18
CH	4% MK	7	1074	25	13,500
CH	4% MK	28	1075	18	12,000
CH	15% MK	7	1137	27	155,000
CH	15% MK	28	1139	78	57,000

5.9. Evaluation of Sustainable Benefits, Life Cycle Assessment, and Service Life Enhancement for Pavement Infrastructure

A sustainable benefit and cost analysis were attempted. However, upon review of the cost of ingredients used to manufacture geopolymer, it was evident that the cost of these ingredients are at a level that when compared to that of cement or lime, an analysis would always lead to the selection of more commonly used products. The reduction of cost of geopolymer is estimated to occur with increase in demand, but this reduction cannot be estimated as many intangible variables are involved. Also, information regarding the distance from the manufacturing unit to the site has significant influence on the cost and sustainable benefits, and future development of manufacturing units of raw materials is difficult to predict. Due to these factors, it is difficult to complete such analysis. A field implementation project involving geopolymer-stabilized soil may be helpful in performing such an analysis.

A hypothetical scenario is presented wherein, as a typical pavement is considered which is built on native high-plasticity soil. The benefits of geopolymer treatment in the form of service life are presented. The traffic criteria assumed for the study and the pavement design characteristics used are given in Table 9 and Table 10, respectively. The annual daily traffic (ADT) data was obtained from the Texas Department of Transportation for a roadway in the Dallas-Fort Worth area, which has significant distress due to presence of expansive soil.

Table 9. Traffic characteristics applied for sustainable benefit study.

Traffic Criteria	Assumption
Annual Daily Traffic (ADT)	2500 vehicles/day
Truck percentage	1.7%
Annual growth in traffic	3%
18-kip Equivalent Single Axle Load (ESAL)	1 million
Initial Serviceability Index	4.5
Final Serviceability Index	3.0
Serviceability Index after overlay	4.2

Table 10. Pavement design characteristics for sustainable benefit study.

Case No.	Hot Mix Asphalt (HMA) Layer Thickness (in.)	Base Layer Thickness (in.)	Stabilized subgrade Thickness (in.)
1	2	8	12
2	3	6	12
3	2	7	12

The control section has a 4-layer system, where the traditionally stabilized subgrade modulus E was assumed to be 22 ksi, while untreated subgrade has a modulus of 11 ksi. For all the cases, the modulus of the geopolymer-stabilized soil was assumed to be 27 ksi. The HMA ($E = 500$ ksi) and base layer ($E = 50$ ksi) properties remain the same as mentioned for each case. A software named FPS-21 was used to perform the analysis to compute service life of pavements. The details regarding the calculation are shown in Appendix A.

From this case study, it was estimated that the use of geopolymer-stabilized subgrade of 12" thickness has approximately 10% increase in the overall service life, with an increase in rutting life of around 13% as compared to those for a typical pavement section which have subgrades stabilized using traditional stabilizers. Hence, geopolymer stabilized subgrade has great potential to enhance the performance of pavement infrastructure built on expansive soils.

6. CONCLUSIONS

Geopolymer has showed promise as stabilizer for clayey soil in terms of volumetric expansion and shrinkage. In terms of UCS, the treated soil showed an increase of up to 400% compare to untreated soil with up to 15% MK. When looking at the trend of strength improvement throughout different %MK, there seems to be a significant increase in strength when increasing the %MK above 4%. It's interesting that the GP treated soil showed significant immediate strength increase within 6 hours of treatment, and then reaches maximum strength within 7 days of treatment. Similarly, the pH test also showed that the treated soil specimens also had a significant increase when %MK is raised above 4%. The trend and results from UCS do match the results from pH test of the different %MK treated soil specimens since GP should have a more completed reaction at higher pH and result in a better strength.

From the parametric study of the GP-soil system for CL, the best-performing parameter combination is concluded to be K431 at 20% water for 4% MK. However, the GP-soil system is complicated and contains many parameters that are dependent on each other. One of the possible ways to improve this study is to go through the various parameters but at a higher %MK, since it is shown that higher %MK past 4% shows significant increase, which can then produce results that are more statistically different and comparable with each other.

Geopolymer-based cement/sand also shows similar behavior to that of GP-soil system in the sense that larger GPC% shows a more significance difference between the different variations. Across the different compositions, the UCS mostly follows the expected trend except for when the mixture does not have enough water to be mixed properly. It's also noted that curing for 14 days under ambient condition is most likely not enough to demonstrate that K-based geopolymer follows the expected trend. For shrinkage, most of the compositions perform on par with OPC with a few showing significant shrinkage. However, the significant shrinkage is not present when these specific compositions are added into sand. Most of the compositions also shows the expected trend in terms of density, porosity, and UCS. On the other hand, when it comes to GPC/sand, most of the expected trends were not observed, this is most likely due to alkali-aggregate reaction, and this will need to be further studied to confirm. From the SEM characterizations, it is shown that GPC has good apparent adhesion with sand particles. But additional characterizations such as *in-situ* indentation testing can provide us a better quantitative understanding.

In terms of durability, more tests are still needed for treated soil specimen and GPC mortar, such as swelling, shrinkage, and leaching tests. The performance of GPC-treated soil clearly demonstrates its effectiveness in stabilizing clayey soils – the quick curing, significant increase in strength, and minimal volumetric changes during 1D-swell and shrinkage tests. GPC shows great potentials to be used as stabilizers where the time for construction is very limited and lowest cost of stabilization is not essential. Future studies on other problematic soils are suggested prior to be considered for field implementations.

REFERENCES

1. Davidovits, J. Geopolymers: inorganic polymeric new materials. *Journal of Thermal Analysis Calorimetry,* Vol. 37, No. 8, 1991, pp. 1633-1656.

2. Phummiphan, I., S. Horpibulsuk, P. Sukmak, A. Chinkulkijniwat, A. Arulrajah, and S.-L. Shen. Stabilisation of marginal lateritic soil using high calcium fly ash-based geopolymer. *Road Materials and Pavement Design,* Vol. 0629, 2016, pp. 1-15.

3. Zhang, M., H. Guo, T. El-Korchi, G. Zhang, and M. Tao. Experimental feasibility study of geopolymer as the next-generation soil stabilizer. *Construction and Building Materials,* Vol. 47, 2013, pp. 1468-1478.

4. Lizcano, M., A. Gonzalez, S. Basu, K. Lozano, and M. Radovic. Effects of water content and chemical composition on structural properties of alkaline activated metakaolin-based geopolymers.In *Journal of the American Ceramic Society,* No. 95, 2012. pp. 2169-2177.

5. Gartner, E. Industrially interesting approaches to "low-CO2" cements. *Cement and Concrete Research,* Vol. 34, No. 9, 2004, pp. 1489-1498.

6. Provis, J. L., and J. S. J. Van Deventer. *Geopolymers: structures, processing, properties and industrial applications*. Elsevier, 2009.

7. McLellan, B. C., R. P. Williams, J. Lay, A. Van Riessen, and G. D. Corder. Costs and carbon emissions for geopolymer pastes in comparison to ordinary portland cement. *Journal of Cleaner Production,* Vol. 19, No. 9-10, 2011, pp. 1080-1090.

8. Das, J. T., A. Banerjee, S. Chakraborty, and A. J. Puppala. A Framework for Assessment of Sustainability and Resilience in Subgrade Stabilization for a High-Volume Road. Presented at *Transportation Research Board 97th Annual Meeting*, Washington D.C., United States, 2018.

9. Das, J. T., A. J. Puppala, T. V. Bheemasetti, L. A. Walshire, and M. K. Corcoran. Sustainability and resilience analyses in slope stabilisation.In *Proceedings of the Institution of Civil Engineers-Engineering Sustainability, No. 171*, Thomas Telford Ltd, 2016. pp. 25-36.

10. He, S., X. Yu, A. Banerjee, and A. J. Puppala. Expansive soil treatment with liquid ionic soil stabilizer. *Transportation Research Record: Journal of the Transportation Research Board,* Vol. 2672, No. 52, 2018, pp. 185-194.

11. Puppala, A. J., D. Basu, O. Cuisinier, and J. T. Das. General Report of TC 307–Sustainability in Geotechnical Engineering. In *Proc. 19th ICSMGE*, 2017, pp. 3353-3360.

12. Puppala, A. J., J. T. Das, T. V. Bheemasetti, and S. S. Congress. Sustainability and Resilience in Transportation Infrastructure Geotechnics: Integrating Advanced Technologies for Better Asset Management. *Geo-Strata—Geo Institute of ASCE,* Vol. 22, No. 3, 2018, pp. 42-48.

13. Correia, A. G., M. Winter, and A. Puppala. A review of sustainable approaches in transport infrastructure geotechnics. *Transportation Geotechnics,* Vol. 7, 2016, pp. 21-28.

14. Talling, B. Geopolymers give fire safety to cruise ships. In *Geopolymers 2002: Turn Potential into Profit*, Melbourne, Australia, 2002.

15. Lyon, R. E., P. Balaguru, A. Foden, U. Sorathia, J. Davidovits, and M. Davidovics. Fire-resistant aluminosilicate composites. *Fire and Materials,* Vol. 21, No. 2, 1997, pp. 67-73.

16. Krivenko, P., and G. Y. Kovalchuk. Directed synthesis of alkaline aluminosilicate minerals in a geocement matrix. *Journal of Materials Science,* Vol. 42, No. 9, 2007, pp. 2944-2952.

17. Van Deventer, J., J. Provis, P. Duxson, and G. Lukey. Reaction mechanisms in the geopolymeric conversion of inorganic waste to useful products. *Journal of Hazardous Materials,* Vol. 139, No. 3, 2007, pp. 506-513.

18. Bagci, C., G. P. Kutyla, K. C. Seymour, and W. M. Kriven. Synthesis and characterization of silicon carbide powders converted from metakaolin-based geopolymer. *Journal of the American Ceramic Society,* Vol. 99, No. 7, 2016, pp. 2521-2530.

19. Salas, D. A., A. D. Ramirez, N. Ulloa, H. Baykara, and A. J. Boero. Life cycle assessment of geopolymer concrete. *Construction and Building Materials,* Vol. 190, 2018, pp. 170-177.

20. Teh, S. H., T. Wiedmann, A. Castel, and J. de Burgh. Hybrid life cycle assessment of greenhouse gas emissions from cement, concrete and geopolymer concrete in Australia. *Journal of Cleaner Production,* Vol. 152, 2017, pp. 312-320.

21. Zhang, M., M. Zhao, G. Zhang, P. Nowak, A. Coen, and M. Tao. Calcium-free geopolymer as a stabilizer for sulfate-rich soils. *Applied Clay Science,* Vol. 108, 2015, pp. 199-207.

22. Pedarla, A., S. Chittoori, and A. J. Puppala. Influence of mineralogy and plasticity index on the stabilization effectiveness of expansive clays. *Transportation Research Record,* Vol. 2212, No. 1, 2011, pp. 91-99.

23. Das, J. T. Evaluation of the rate of secondary swelling in expansive clays using centrifuge technology. In *No. Master of Science in Engineering*, University of Texas at Austin, Austin, Texas, 2014.

24. Banerjee, A., A. Puppala, L. R. Hoyos, W. Likos, and U. Patil. Resilient Modulus of Expansive Soils at High Suction Using Vapor Pressure Control. *Geotechnical Testing Journal*, 2020, 43(2) pp. 1-17 (In-press).

25. Banerjee, A., A. Puppala, U. Patil, L. Hoyos, and P. Bhaskar. A simplified approach to determine the response of unsaturated soils using multistage triaxial test. *IFCEE 2018: Advances in Geomaterial Modeling and Site Characterization, GSP,* Vol. 295, 2018, pp. 332-342.

26. Petry, T. M., and D. N. Little. Review of stabilization of clays and expansive soils in pavements and lightly loaded structures—history, practice, and future. *Journal of Materials in Civil Engineering,* Vol. 14, No. 6, 2002, pp. 447-460.

27. Puppala, A. J., S. S. Congress, and A. Banerjee. Research advancements in expansive soil characterization, stabilization and geoinfrastructure monitoring. In *Frontiers in Geotechnical Engineering*, Springer, 2019. pp. 15-29.

28. Puppala, A. J., T. Manosuthkij, S. Nazarian, and L. R. Hoyos. Threshold moisture content and matric suction potentials in expansive clays prior to initiation of cracking in pavements. *Canadian Geotechnical Journal,* Vol. 48, No. 4, 2011, pp. 519-531.

29. Banerjee, A., U. D. Patil, A. J. Puppala, and L. R. Hoyos. Suction-controlled repeated load triaxial test of subgrade soil at high suction states. In *Unsaturated Soils, Proceeding of Seventh International Conference on Unsaturated Soils. Hong Kong, China: HKUST*, 2018. pp. 667-672.

30. George, A. M., S. Chakraborty, J. T. Das, A. Pedarla, and A. J. Puppala. Understanding shallow slope failures on expansive soil embankments in north Texas using unsaturated soil property framework. Presented at *PanAm Unsaturated Soils 2017*, Dallas, TX, 2017.

31. Madhyannapu, R. S., and A. J. Puppala. Design and construction guidelines for deep soil mixing to stabilize expansive soils. *Journal of Geotechnical and Geoenvironmental Engineering,* Vol. 140, No. 9, 2014.

32. Madhyannapu, R. S., A. J. Puppala, S. Nazarian, and D. Yuan. Quality assessment and quality control of deep soil mixing construction for stabilizing expansive subsoils. *Journal of Geotechnical and Geoenvironmental Engineering,* Vol. 136, No. 1, 2009, pp. 119-128.

33. Puppala, A., and S. Hanchanloet. Evaluation of a new chemical (SA-44/LS-40) treatment method on strength and resilient properties of a cohesive soil.In *78th Annual Meeting of the Transportation Research Board,* Washington, D.C., 1999.

34. Puppala, A. J., E. Wattanasanticharoen, and L. R. Hoyos. Ranking of four chemical and mechanical stabilization methods to treat low-volume road subgrades in Texas. *Transportation Research Record,* Vol. 1819, No. 1, 2003, pp. 63-71.

35. Chakraborty, S., and S. Nair. Impact of curing time on moisture-induced damage in lime-treated soils. *International Journal of Pavement Engineering*, 2018, pp. 1-13.

36. Chakraborty, S., and S. Nair. Impact of different hydrated cementitious phases on moisture-induced damage in lime-stabilised subgrade soils. *Road Materials and Pavement Design,* Vol. 19, No. 6, 2018, pp. 1389-1405.

37. Caballero, S., R. Acharya, A. Banerjee, T. V. Bheemasetti, A. Puppala, and U. Patil. Sustainable slope stabilization using biopolymer-reinforced soil. *Geo-Chicago,* ASCE Library: Reston, VA, USA, 2016.

38. Biswas, N., and P. Ghosh. Interaction of adjacent strip footings on reinforced soil using upper-bound limit analysis. *Geosynthetics International,* Vol. 25, No. 6, 2018, pp. 599-611.

39. Biswas, N., and P. Ghosh. Bearing Capacity Factors for Isolated Surface Strip Footing Resting on Multi-layered Reinforced Soil Bed. *Indian Geotechnical Journal,* Vol. 49, No. 1, 2019, pp. 37-49.

40. Banerjee, A. Response of unsaturated soils under monotonic and dynamic loading over moderate suction states.In *Department of Civil Engineering, Doctor of Philosophy Dissertation*, The University of Texas at Arlington, Arlington, TX, 2017.

41. Chittoori, B. C., A. J. Puppala, T. Wejrungsikul, and L. R. Hoyos. Experimental studies on stabilized clays at various leaching cycles. *Journal of Geotechnical and Geoenvironmental Engineering,* Vol. 139, No. 10, 2013, pp. 1665-1675.

42. Zhang, M. Geopolymer, Next Generation Sustainable Cementitious Material− Synthesis, Characterization and Modeling. In *Civil and Environmental Engineering, No. Doctor of Philosophy*, Worcester Polytechnic Institute, 2015. p. 298.

43. Adhikari, S. *Mechanical Properties of Soil-RAP-Geopolymer for the Stabilization of Road Base/Subbase*. University of Louisiana at Lafayette, 2017.

44. Hardjito, D., S. Wallah, D. Sumajouw, and B. Rangan. Introducing fly ash-based geopolymer concrete: manufacture and engineering properties. In *30th conference on our world in concrete & structures*, 2005. pp. 23-24.

45. Hardjito, D., S. E. Wallah, D. M. Sumajouw, and B. V. Rangan. On the development of fly ash-based geopolymer concrete. *Materials Journal,* Vol. 101, No. 6, 2004, pp. 467-472.

46. Hardjito, D., S. E. Wallah, D. M. J. Sumajouw, and B. V. Rangan. Factors Influencing the Compressive Strength of Fly Ash-Based Geopolymer Concrete. *Civil Engineering Dimension,* Vol. 6, 2004, pp. pp. 88-93.

47. Shayan, A. Specification and use of geopolymer concrete in the manufacture of structural and non-structural components: review of literature. No. AP-T318-16. 2016.

48. Vaidya, S., E. Diaz, and E. Allouche. Experimental evaluation of self-cure geopolymer concrete for mass pour applications. In *World of coal ash (woca) conference–may*, 2011. pp. 9-12.

49. Glasby, T., J. Day, R. Genrich, and J. Aldred. EFC geopolymer concrete aircraft pavements at Brisbane West Wellcamp Airport. Presented at Concrete 2015, Melbourne, Australia, 2015.

50. Duxson, P., G. C. Lukey, and J. S. J. van Deventer. Physical evolution of Na-geopolymer derived from metakaolin up to 1000 °C. *Journal of Materials Science,* Vol. 42, 2007, pp. 3044-3054.

51. Mo, B.-h., H. Zhu, X.-m. Cui, Y. He, and S.-y. Gong. Effect of curing temperature on geopolymerization of metakaolin-based geopolymers. *Applied Clay Science,* Vol. 99, 2014, pp. 144-148.

52. White, C. E., J. L. Provis, T. Proffen, and J. S. Van Deventer. The effects of temperature on the local structure of metakaolin-based geopolymer binder: A neutron pair distribution function investigation. *Journal of the American Ceramic Society,* Vol. 93, No. 10, 2010, pp. 3486-3492.

53. Zhang, B., K. J. MacKenzie, and I. W. Brown. Crystalline phase formation in metakaolinite geopolymers activated with NaOH and sodium silicate. *Journal of Materials Science,* Vol. 44, No. 17, 2009, pp. 4668-4676.

54. Bell, J. L., P. E. Driemeyer, and W. M. Kriven. Formation of ceramics from metakaolin-based geopolymers. Part II: K-based geopolymer. *Journal of the American Ceramic Society,* Vol. 92, No. 3, 2009, pp. 607-615.

55. Duxson, P., J. L. Provis, G. C. Lukey, F. Separovic, and J. S. van Deventer. 29Si NMR study of structural ordering in aluminosilicate geopolymer gels. *Langmuir,* Vol. 21, No. 7, 2005, pp. 3028-3036.

56. Lizcano, M., H. S. Kim, S. Basu, and M. Radovic. Mechanical properties of sodium and potassium activated metakaolin-based geopolymers. *Journal of Materials Science,* Vol. 47, 2012, pp. 2607-2616.

57. Rowles, M., and B. O'Connor. Chemical optimisation of the compressive strength of aluminosilicate geopolymers synthesised by sodium silicate activation of metakaolinite. *Journal of Materials Chemistry,* Vol. 13, No. 5, 2003, pp. 1161-1165.

58. Zhang, M., M. Zhao, G. Zhang, T. El-Korchi, and M. Tao. A multiscale investigation of reaction kinetics, phase formation, and mechanical properties of metakaolin geopolymers. *Cement and Concrete Composites,* Vol. 78, 2017, pp. 21-32.

59. Subaer, and A. van Riessen. Thermo-mechanical and microstructural characterisation of sodium-poly(sialate-siloxo) (Na-PSS) geopolymers. *Journal of Materials Science,* Vol. 42, No. 9, 2007, pp. 3117-3123.

60. Marín-López, C., J. L. Reyes Araiza, A. Manzano-Ramírez, J. C. Rubio Avalos, J. J. Perez-Bueno, M. S. Muñiz-Villareal, E. Ventura-Ramos, and Y. Vorobiev. Synthesis and characterization of a concrete based on metakaolin geopolymer. *Inorganic Materials,* Vol. 45, No. 12, 2009, pp. 1429-1432.

61. Olivia, M., and H. Nikraz. Properties of fly ash geopolymer concrete designed by Taguchi method. *Materials & Design (1980-2015),* Vol. 36, 2012, pp. 191-198.

62. Škvára, F., V. Šmilauer, P. Hlaváček, L. Kopecký, and Z. Cílová. A weak alkali bond in (N, K)-A-S-H gels: Evidence from leaching and modeling. *Ceramics - Silikaty,* Vol. 56, 2012, pp. 374-382.

63. Horpibulsuk, S., C. Suksiripattanapong, W. Samingthong, R. Rachan, and A. Arulrajah. Durability against wetting–drying cycles of water treatment sludge–fly ash geopolymer and water treatment sludge–cement and silty clay–cement systems. *Journal of Materials in Civil Engineering,* Vol. 28, No. 1, 2015.

64. Fernández-Jiménez, A., I. García-Lodeiro, and A. Palomo. Durability of alkali-activated fly ash cementitious materials. *Journal of Materials Science,* Vol. 42, No. 9, 2007, pp. 3055-3065.

65. Bakharev, T., J. Sanjayan, and Y.-B. Cheng. Resistance of alkali-activated slag concrete to carbonation. *Cement and Concrete Research,* Vol. 31, No. 9, 2001, pp. 1277-1283.

66. Criado, M., A. Palomo, and A. Fernández-Jiménez. Alkali activation of fly ashes. Part 1: Effect of curing conditions on the carbonation of the reaction products. *Fuel,* Vol. 84, No. 16, 2005, pp. 2048-2054.

67. Bernal, S. A., R. San Nicolas, J. L. Provis, R. M. De Gutiérrez, and J. S. van Deventer. Natural carbonation of aged alkali-activated slag concretes. *Materials and Structures,* Vol. 47, No. 4, 2014, pp. 693-707.

68. Bernal, S. A., J. L. Provis, D. G. Brice, A. Kilcullen, P. Duxson, and J. S. van Deventer. Accelerated carbonation testing of alkali-activated binders significantly underestimates service life: The role of pore solution chemistry. *Cement and Concrete Research,* Vol. 42, No. 10, 2012, pp. 1317-1326.

69. Van Jaarsveld, J., J. Van Deventer, and G. Lukey. The characterisation of source materials in fly ash-based geopolymers. *Materials Letters,* Vol. 57, No. 7, 2003, pp. 1272-1280.

70. Phair, J., and J. Van Deventer. Effect of silicate activator pH on the leaching and material characteristics of waste-based inorganic polymers. *Minerals Engineering,* Vol. 14, No. 3, 2001, pp. 289-304.

71. Fernando, P.-T., and J. Said. Resistance to acid attack, abrasion and leaching behavior of alkali-activated mine waste binders. *Materials and Structures,* Vol. 44, No. 2, 2011, pp. 487-498.

72. García-Lodeiro, I., A. Palomo, and A. Fernández-Jiménez. Alkali–aggregate reaction in activated fly ash systems. *Cement and Concrete Research,* Vol. 37, No. 2, 2007, pp. 175-183.

73. Lloyd, R. R., J. L. Provis, and J. S. Van Deventer. Pore solution composition and alkali diffusion in inorganic polymer cement. *Cement and Concrete Research,* Vol. 40, No. 9, 2010, pp. 1386-1392.

74. Pacheco-Torgal, F., Z. Abdollahnejad, A. Camões, M. Jamshidi, and Y. Ding. Durability of alkali-activated binders: a clear advantage over Portland cement or an unproven issue? *Construction and Building Materials,* Vol. 30, 2012, pp. 400-405.

75. Reddy, D. V., J.-B. Edouard, and K. Sobhan. Durability of fly ash–based geopolymer structural concrete in the marine environment. *Journal of Materials in Civil Engineering,* Vol. 25, No. 6, 2012, pp. 781-787.

76. ASTM. Standard Specification for Standard Sand. In *No. C778-17*, ASTM International, West Conshohocken, PA, 2017.

77. ASTM. Standard Test Method for Compressive Strength of Hydraulic Cement Mortars (Using 2-in. or [50-mm] Cube Specimens). In *No. C109 / C109M-16a*, ASTM International, West Conshohocken, PA, 2016.

78. ASTM. Standard Test Methods for Apparent Porosity, Liquid Absorption, Apparent Specific Gravity, and Bulk Density of Refractory Shapes by Vacuum Pressure. In *No. ASTM C830 - 00*, ASTM International, West Conshohocken, PA, 2016.

79. ASTM. Standard Test Methods for Liquid Limit, Plastic Limit, and Plasticity Index for Soils.In*, No. D4318-17e1*, ASTM International, West Conshohocken, PA, 2017.

80. ASTM. Standard Test Methods for Specific Gravity of Soil Solids by Water Pycnometer.In*, No. D854-14*, ASTM International, West Conshohocken, PA, 2014.

81. ASTM. Standard Test Methods for Laboratory Compaction Characteristics of Soil Using Standard Effort (12400 ft-lbf/ft3 (600 kN-m/m3)). In *No. D698-12e2*, ASTM International, West Conshohocken, PA, 2012.

82. Scavuzzo, R. Use of the Harvard Miniature Apparatus for obtaining moisture-unit weight relationships of soils. In U.S. Department of Interior, Bureau of Reclamation, Denver, CO, 1984.

83. Huang, O. D., R. Samuel, A. Banerjee, A. J. Puppala, and M. Radovic. Development of Alternative Stabilization Methods for Transportation Infrastructure Based on Geopolymers.In *MATEC Web of Conferences, No. 271*, EDP Sciences, 2019.

84. Samuel, R., O. Huang, A. Banerjee, A. Puppala, J. Das, and M. Radovic. Case Study: Use of Geopolymers to Evaluate the Swell-Shrink Behavior of Native Clay in North Texas.In *Eighth International Conference on Case Histories in Geotechnical Engineering (Geo-Congress 2019) American Society of Civil Engineers*, 2019.

85. Xu, H., and J. Van Deventer. The geopolymerisation of alumino-silicate minerals. *International Journal of Mineral Processing,* Vol. 59, No. 3, 2000, pp. 247-266.

86. ASTM. Standard Test Methods for Wetting and Drying Compacted Soil-Cement Mixtures.In*, No. D559 / D559M-15*, ASTM International, West Conshohocken, PA, 2015.

87. McCallister, L. The effects of leaching on lime-stabilized expansive clays.In, Doctoral thesis, The University of Texas at Arlington, TX, 1990.

88. Chittoori, B. C. S. Clay mineralogy effects on long-term performance of chemically treated expansive clays. 2009.

89. Lizcano, M. Effects of water content and alumino-silicate sources on the structure and properties of geopolymers. PhD disserttion, Texas A&M University, 2011.

90. Barsoum, M., and M. Barsoum. *Fundamentals of ceramics*. CRC press, 2002.

91. Chakraborty, S., T. V. Bheemasetti, A. J. Puppala, and S. Nazarian. A rational approach to select the number of field tests required to determine subgrade properties. *International Journal of Pavement Engineering*, 2017, pp. 1-9.

92. Duxson, P., A. Fernández-Jiménez, J. L. Provis, G. C. Lukey, A. Palomo, and J. S. J. Van Deventer. Geopolymer technology: The current state of the art. *Journal of Materials Science,* Vol. 42, 2007, pp. 2917-2933.

93. Banerjee, A., and A. Puppala. Influence of Rate of Shearing on Strength Characteristics of Saturated and Unsaturated Silty Soil. In *Proc. 50th Indian Geotechnical Conference*, 2015.

APPENDIX A: SUSTAINABLE BENEFITS STUDY

The benefits of Geopolymer treatment in the form of service life are presented in this section. A hypothetical scenario is presented, as a typical pavement is considered which is built on native high-plasticity soil.

A.1. Traffic Data and Basic Design Criteria

The traffic characteristics assumed for the study are as follows:

- ADT = 2500 vehicles/day;
- Truck percentage = 1.7%;
- Annual growth in traffic = 3%;
- 18-kip ESAl = 1 million;
- Initial Serviceability Index = 4.5;
- Final Serviceability Index = 3.0; and
- Serviceability Index after overlay = 4.2.

Three designs have been considered for this case study as follows:

1. HMA layer 2" thick; Base layer 8" thick; Stabilized subgrade 12" thick;
2. HMA layer 3" thick; Base layer 6" thick; Stabilized subgrade 12" thick; and
3. HMA layer 2" thick; Base layer 7" thick; Stabilized subgrade 12" thick.

The control section also has a 4-layer system, where for the traditionally stabilized subgrade modulus *E* was assumed to be 22 ksi, while untreated subgrade has a modulus of 11 ksi. For all the cases, the modulus of the geopolymer-stabilized soil was assumed to be 27 ksi. The HMA (*E* = 500 ksi) and base layer (*E* = 50 ksi) properties remain the same as mentioned for each case.

The details of each case are presented below.

A.2. Case Study Results

A.2.1. Case 1: HMA Layer 2" Thick, Base Layer 8" Thick

Pavement thickness and material properties:

- HMA – 2" (E = 500 ksi);
- Base Material – 8" (E = 50 ksi);
- Stabilized Subgrade – 12" (E = 27 ksi for Geopolymer stabilized soil and E = 22 ksi for traditionally stabilized soil); and
- Subgrade below these layers (E = 11 ksi).

Geopolymer stabilized section:

- Service Life = 12.5 years (without overlay) and 23.4 years (with 2" overlay);
- Traffic to first overlay = 0.552 million ESALs;
- Crack life = 0.59 million ESALs; and
- Rutting Life = 4.51 million ESALs.

Traditionally stabilized section (current practice):

- Service Life = 11.4 years (without overlay) and 21.6 years (with 2" overlay);

- Traffic to first overlay = 0.497 million ESALs;
- Crack life = 0.57 million ESALs; and
- Rutting Life = 3.96 million ESALs.

As compared to traditionally stabilized soil, an increase in service life from 11.4 years to 12.5 years (without overlay), which accounts for a 9.6% increase, was predicted in the case of geopolymer-stabilized soil. Rutting life was also estimated to increase by 13.9%.

A.2.2. Case 2: HMA Layer 3" Thick, Base Layer 6" Thick

Pavement thickness and material properties:

- HMA – 3" (E = 500 ksi);
- Base Material – 6" (E = 50 ksi);
- Stabilized Subgrade – 12" (E = 27 ksi for Geopolymer stabilized soil and E = 22 ksi for traditionally stabilized soil); and
- Subgrade below these layers (E = 11 ksi).

Geopolymer stabilized section:

- Service Life = 13.5 years (without overlay) and 25.2 years (with 2" overlay);
- Traffic to first overlay = 0.611 million ESALs;
- Crack life = 0.82 million ESALs; and
- Rutting Life = 3.86 million ESALs.

Traditionally stabilized section (current practice):

- Service Life = 12.3 years (without overlay) and 23.1 years (with 2" overlay);
- Traffic to first overlay = 0.542 million ESALs;
- Crack life = 0.75 million ESALs; and
- Rutting Life = 3.45 million ESALs.

As compared to traditionally stabilized soil, an increase in service life from 12.3 years to 13.5 years (without overlay), which accounts for a 9.8% increase, was predicted in the case of geopolymer-stabilized soil. Rutting life was also predicted to increase by 11.9%.

A.2.3. Case 3: HMA Layer 2" Thick, Base Layer 7" Thick

Pavement thickness and material properties:

- HMA – 2" (E = 500 ksi);
- Base Material – 7" (E = 50 ksi);
- Stabilized Subgrade – 12" (E = 27 ksi for Geopolymer stabilized soil and E = 22 ksi for traditionally stabilized soil); and
- Subgrade below these layers (E = 11 ksi).

Geopolymer stabilized section:

- Service Life = 11.7 years (without overlay) and 22.0 years (with 2" overlay);
- Traffic to first overlay = 0.511 million ESALs;
- Crack life = 0.57 million ESALs; and
- Rutting Life = 3.21 million ESALs.

Traditionally stabilized section (current practice):

- Service Life = 10.5 years (without overlay) and 20.0 years (with 2" overlay);
- Traffic to first overlay = 0.452 million ESALs;
- Crack life = 0.55 million ESALs; and
- Rutting Life = 2.81 million ESALs.

As compared to traditionally stabilized soil, an increase in service life from 10.5 years to 11.7 years (without overlay), which accounts for a 11.4% increase. Rutting life was also predicted to increase by 14.2%.

A.3. Conclusion

From this study, it was observed that the use of geopolymer-stabilized subgrade of 12" thickness has approximately 10% increase in the overall service life of a typical pavement as described above, with an increase in rutting life of around 13%. Hence, geopolymer stabilized subgrade has great potential to enhance the performance of pavement infrastructure built on expansive